CANADIAN JOURNAL OF RESEARCH

VOLUME 20 JUNE, 1942 NUMBER 6

CONTENTS

SECTION A.—PHYSICAL SCIENCES

SECTION B.—CHEMICAL SCIENCES

NATIONAL RESEARCH COUNCIL
OTTAWA, CANADA

Publications and Subscriptions

The Canadian Journal of Research is issued monthly in four sections, as follows:

A. Physical Sciences
B. Chemical Sciences
C. Botanical Sciences
D. Zoological Sciences

For the present, Sections A and B are issued under a single cover, as also are Sections C and D, with separate pagination of the four sections, to permit separate binding, if desired.

Subscription rates, postage paid to any part of the world (effective 1 April, 1939), are as follows:

	Annual	*Single Copy*
A and B	$ 2.50	$ 0.50
C and D	2.50	0.50
Four sections, complete	4.00	—

The Canadian Journal of Research is published by the National Research Council of Canada under authority of the Chairman of the Committee of the Privy Council on Scientific and Industrial Research. All correspondence should be addressed:

National Research Council, Ottawa, Canada.

Notice to Contributors

Fifty reprints of each paper are supplied free. Additional reprints, if required, will be supplied according to a prescribed schedule of charges.

Reprinted in entirety by photo-offset.

Canadian Journal of Research

Issued by THE NATIONAL RESEARCH COUNCIL OF CANADA

VOL. 20, SEC. A. JUNE, 1942 NUMBER 6

BAND SPECTRUM AND STRUCTURE OF THE CH^+ MOLECULE; IDENTIFICATION OF THREE INTERSTELLAR LINES[1]

BY A. E. DOUGLAS[2] AND G. HERZBERG[3]

Abstract

In a discharge through helium, to which a small trace of benzene vapour is added, a new band system of the type $^1\Pi - {}^1\Sigma$ is found which is shown to be due to the CH^+ molecule. The $R(0)$ lines of the 0–0, 1–0, and 2–0 bands of the new system agree exactly with the hitherto unidentified interstellar lines 4232.58, 3957.72, 3745.33 Å, thus proving that CH^+ is present in interstellar space. At the same time this observation of the band system in absorption shows that the lower state $^1\Sigma$ is the ground state of the CH^+ molecule. The new bands are closely analogous to the $^1\Pi - {}^1\Sigma^+$ BH bands. The analysis of the bands leads to the following vibrational and rotational constants of CH^+ in its ground state: $\Delta G_{\frac{1}{2}}'' = 2739.54$, $B_e'' = 14.1767$, $\alpha_e'' = 0.4898$ cm.$^{-1}$. The internuclear distance is $r_e'' = 1.1310 \cdot 10^{-8}$ cm. (for further molecular constants see Table V). From the vibrational levels of the upper $^1\Pi$ state the heat of dissociation of CH^+ can be obtained within fairly narrow limits: $D_0(CH^+) = 3.61 \pm 0.22$ e.v. From this value the ionization potential of CH is derived to be $I(CH) = 11.13 \pm 0.22$ e.v. The bearing of this value on recent work on ionization and dissociation of polyatomic molecules by electron impacts is briefly discussed.

A. Introduction

The work of Swings and Rosenfeld (22) and McKellar (14, 15, 16) has shown definitely that certain interstellar lines found by Dunham and Adams (6, 5, 1) are due to the absorption by CH and CN (and possibly NaH) molecules present in interstellar space. Since these interstellar molecules are practically undisturbed by collisions with other molecules or atoms, if they have once been excited they will radiate all their energy and in general go over into the very lowest state (electronic, vibrational, and rotational) before they will absorb another quantum. That is why only single sharp lines, rather than bands, are observed which agree with those lines of the laboratory bands that have the lowest (or in two cases the second lowest) rotational and vibrational level of the ground state as their lower state.

Apart from the mysterious diffuse interstellar bands found by Merrill and Wilson (17, 18) and Beals and Blanchet (3) four sharp interstellar lines 3579.04, 3745.33, 3957.72, 4232.58 Å remained unexplained. Since they could hardly be atomic in origin and since they fitted none of the absorption

[1] *Manuscript received February 26, 1942.*

Contribution from the Department of Physics, University of Saskatchewan, Saskatoon, Sask., with financial assistance from the National Research Council of Canada.

[2] *Physicist, National Research Laboratories, Ottawa.*

[3] *Research Professor of Physics.*

spectra of known molecules, as has been carefully checked by McKellar (16)*, Swings† at a recent conference held at the Yerkes Observatory suggested that they might be due to some molecular ion such as CN^+, CH^+, NO^+ . . . . while Mulliken† suggested the CH_2 molecule. For a number of reasons which need not be given here, Teller and Herzberg‡ concluded that of these possibilities CH^+ was the most likely one. However, at the time, no spectrum of any of the suggested molecules was known.

We therefore thought it worth while to try to find a spectrum of CH^+. In what follows we report the observation of such a spectrum to which three of the four interstellar lines mentioned above belong. Thus these interstellar lines have been definitely identified and information about the structure of the CH^+ molecule has been obtained [compare our preliminary note (4)].

B. Experimental

The new bands here to be discussed were first found in the spectrum of an electrodeless discharge through helium mixed with a small trace of benzene vapour and excited by a powerful high frequency oscillator. However, it was soon found that an ordinary uncondensed discharge with electrodes constitutes an equally good or even better source. Fig. 1 shows relevant parts of the spectrum of the latter source obtained with the Saskatoon 6 m. grating. It may be mentioned that the spectrograms were taken when the colour of the discharge was almost wholly that characteristic of helium. The Swan bands of C_2, which on first admitting the benzene to the helium are very strong, were comparatively weak when the spectra were taken. On the other hand, the CH bands occur very strongly on the spectrograms. The exposure time for the stronger bands was only about one hour, while, for the weaker bands, exposures up to 10 hr. were necessary.

The measurements, mostly of second order plates, were made with a Gaertner comparator. The absolute accuracy of the wave-lengths (referred to iron standards) is estimated to be better than ± 0.01 Å, while the relative accuracy is probably ± 0.003 Å or better.

C. Band Analysis

The rotational and vibrational analysis of the new bands did not offer any difficulty. All the bands are shaded to the red. Each band, as shown by Fig. 1, consists of three branches which are readily identified as P, Q, and R branches. Of these the P branch is the weakest. Unless there is some unresolved fine structure the band system must therefore represent a $^1\Pi - {}^1\Sigma$ or a $^1\Sigma - {}^1\Pi$ transition. The fact that the line $R(0)$ is present while $P(1)$ is absent shows that the transition is $^1\Pi - {}^1\Sigma$, and at the same time

* *We are greatly indebted to Dr. McKellar for sending us a copy of his paper in advance of publication.*

† *Paper at conference on interstellar lines, held at the Yerkes Observatory in June 1941; see the summary by Ledoux (12).*

‡ *Discussion at the Yerkes Conference; see Ledoux (12).*

PLATE I

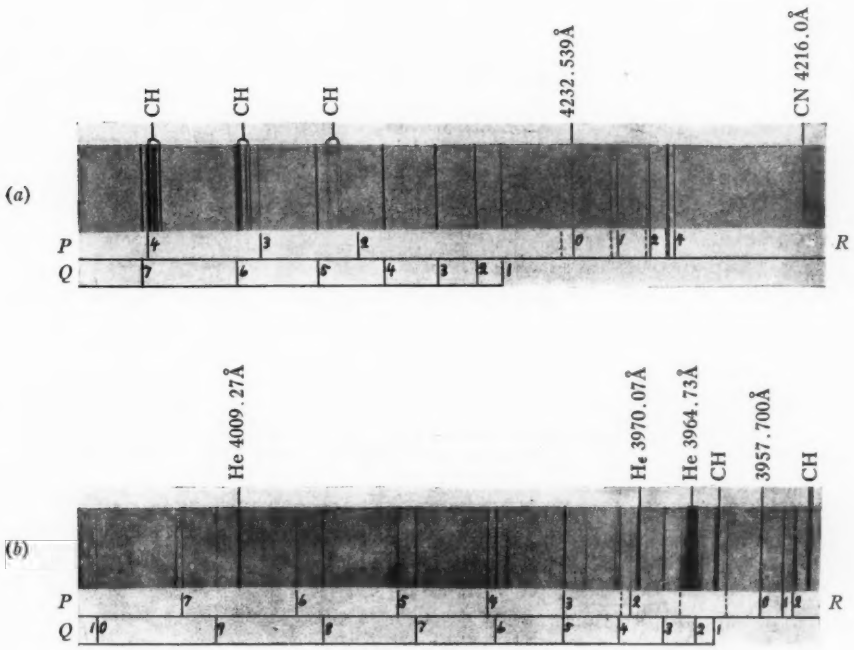

FIG. 1. CH^+ *bands, (a) 0–0 band, (b) 1–0 band. The broken leading lines refer to lines of the returning part of the R branch.*

excludes the possibility $^1\Pi - {}^1\Delta$ or $^1\Delta - {}^1\Pi$ which, except for more missing lines near the origin, would give a similar structure if the Λ doubling is small. A multiplet $\Pi - \Sigma$ transition would have the same structure as observed if the multiplet splitting were unresolved. However, as far as we are aware, no multiplet $\Pi - \Sigma$ bands of molecules other than H_2 or He_2 are known which under such a high dispersion as used here show no splitting. Therefore we consider it as proved that the new bands are $^1\Pi - {}^1\Sigma$ bands.

TABLE I

DESLANDRES TABLE OF THE CH^+ BANDS

ν_0 = wave number of zero line
ν_H = wave number of band head (R branch)

v' \ v''	0	1
0	ν_0 = 23596.94 cm.$^{-1}$ ν_H = 23660.52	ν_0 = 20857.40 cm.$^{-1}$ ν_H = 20932.72
1	ν_0 = 25239.10 ν_H = 25281.35	•
2	ν_0 = 26673.40 ν_H = 26704.14	

* *The 1–1 band appears faintly on a number of plates but it was too weak and too strongly overlapped to be measured.*

In Table I a Deslandres table of the observed bands is given. In spite of a good deal of effort we have been unable to extend the band system further. We tried particularly to find the 3–0 band since it appeared likely that the fourth hitherto unidentified interstellar line λ3579.04 belongs to this band. However, with our source there occur in the same region the $\Delta v = 1$ sequences of the Deslandres-d'Azambuja bands of C_2 and of the violet CN bands consisting of a large number of lines which make an unambiguous identification of a weak CH^+ band impossible. Neither have we been able to find the 3–1 band (which would be sufficient to fix the position of the $v' = 3$ level) even though its expected position is in a more favourable spectral region.

In Table II are given the wave numbers of all the band lines of the CH^+ system with the assignment of the J values. None of the bands extends to very high J values. The J values are also indicated on the spectrograms of the 0–0 and 1–0 bands in Fig. 1, where it is seen that the numbering chosen is obvious. Table III gives the combination differences $\Delta_2 F''(J)$ for the 0–0, 1–0, and 2–0 bands which agree very satisfactorily. On the other hand, there is a systematic difference between the $\Delta_1 F'(J)$ values calculated from $R(J) - Q(J)$ and those calculated from $Q(J+1) - P(J+1)$ of each band, indicating a not negligible Λ type doubling in the upper $^1\Pi$ state. The rotational constants for the upper levels of the Q branches were therefore evaluated independently from those of the P and R branches.

TABLE II

WAVE NUMBERS OF BAND LINES

J	0–0 Band			1–0 Band			2–0 Band			0–1 Band*		
	R(J)	Q(J)	P(J)	R(J)	Q(J)	P(J)	R(J)	Q(J)	P(J)	R(J)	Q(J)	P(J)
0	23619.85			25259.97			26692.50			20880.27		
1	637.71	23591.89		274.22	25232.20		702.76	26664.57		899.13	20853.31	
2	650.48	581.77	23536.26	281.35	218.28	25176.62	704.14	646.91	26608.99	913.83	845.18	20799.88
3	658.14	566.56	498.57	281.35	197.43	135.10	696.61	620.41	563.69	924.37	832.88	764.90
4	660.52	546.23	455.87	274.22	169.54	086.80	679.95	584.88	509.67	930.77	816.50	726.24
5	657.55	520.70	408.37	259.97	134.50	031.62	654.10	540.36	446.89	932.72	795.85	683.39
6	649.10	489.92		237.93	092.35	24969.61	618.86	486.79	375.35	930.08	770.87	636.84
7	635.01	453.76		208.57	042.86	900.63	574.17	423.95	294.96		741.57	
8		412.16		171.36	24985.95	824.68	519.77	351.82	205.56		707.73	
9				126.22	921.48			270.18				
10					849.28			178.85				
11					769.27							

* *This band was measured on a first order spectrogram. The wave numbers are therefore somewhat less accurate than those of the other bands which were measured on second order spectrograms.*

TABLE III

COMBINATION DIFFERENCES $\Delta_2F''(J)$ FOR THE 0–0, 1–0, AND 2–0 BANDS

J	$\Delta_2F''(J) = R(J-1) - P(J+1)$		
	0–0 Band	1–0 Band	2–0 Band
1	83.59	83.35	83.51
2	139.14	139.12	139.07
3	194.61	194.55	194.47
4	249.77	249.73	249.72
5		304.61	304.60
6		359.34	359.14
7		413.25	413.30

D. Rotational and Vibrational Constants

In Table IV the rotational constants B_v and D_v, as calculated from the observed bands, are given. The constants B_0'' and D_0'' were obtained in the usual way [see Herzberg (9)] from the average of the $\Delta_2F''(J)$ values given in Table III. The B and D values for the upper states of the Q branches B_v^Q and D_v^Q were obtained by determining $B' - B''$ and $D' - D''$ from the plot $Q(J)$ against $J(J+1)$ and assuming the B_0'' and D_0'' value obtained before. This same method also yielded B_1''. The B and D values for the upper states of the P and R branches B_v^{PR} and D_v^{PR} were obtained both from the $\Delta_2F'(J) = R(J) - P(J)$ and by plotting* $R(J-1) + P(J)$ against J^2. The values given in Table IV are the averages of the values obtained in the two ways.

TABLE IV

ROTATIONAL CONSTANTS OF CH^+

v	Upper state, $^1\Pi$				Ground state, $^1\Sigma^+$	
	B_v^Q, cm.$^{-1}$	B_v^{PR}, cm.$^{-1}$	$B_v^{average}$, cm.$^{-1}$	$D_v^{average}$, cm.$^{-1}$	B_v'', cm.$^{-1}$	D_v'', cm.$^{-1}$
0	11.4088	11.4482	11.4285	0.00199	13.9318	0.00139
1	10.4691	10.5010	10.4850	0.00211	13.4420	0.00136
2	9.5206	9.5488	9.5347	0.00214		

As is well-known, for $^1\Pi$ states the Λ type doubling is given by

$$\Delta\nu_{dc}(J) = qJ(J+1) \qquad (1)$$

where q is the difference between the B_v^Q and the B_v^{PR} values. This difference is quite appreciable in the present case. We have for $v' = 0$: $q_0 = 0.0394$ cm.$^{-1}$, for $v' = 1$: $q_1 = 0.0319$ cm.$^{-1}$, and for $v' = 2$: $q_2 = 0.0282$ cm.$^{-1}$. Thus q decreases with increasing v'. It is significant that $B_v^{PR} > B_v^Q$, as would be expected if the splitting is produced by the interaction of the $^1\Pi$ state with the lower $^1\Sigma^+$ state.

* *It may be noticed that a misprint occurs in Herzberg (9, p. 204): The D correction is not* $-2(D'-D'')J^2(J+1)^2$ *but* $-2(D'-D'')J^2(J^2+1)$.

Since the D_v^Q and D_v^{PR} values for the $^1\Pi$ state were found to be the same within the accuracy of the determinations only their average values are given in Table IV.

For the ground state the available data do not allow any conclusions about a possible curvature of the B_v versus v curve. In the upper state the B_v^Q, the B_v^{PR}, as well as the average B_v values show definitely the presence of a negative quadratic term in the formula

$$B_v = B_e - \alpha_e(v + \tfrac{1}{2}) + \gamma_e(v + \tfrac{1}{2})^2. \qquad (2)$$

The B_e'', α_e'', B_e', α_e', γ_e' values obtained from the B_v'' and $B_v'^{(\text{average})}$ are given together with other constants in Table V. Assuming that the emitter of the bands is CH^+ (see Section *E*) we obtain from the B_e values the internuclear distances r_e, also given in Table V.

For the lower state only the first vibrational quantum $\Delta G_{\frac{1}{2}}''$ but not ω_e'' and $\omega_e''x_e''$ can be obtained. For the upper state the values of ω_e' and $\omega_e'x_e'$ resulting from the zero lines in Table I are given in Table V.

TABLE V

MOLECULAR CONSTANTS OF CH^+

	Upper state, $^1\Pi$	Ground state, $^1\Sigma^+$
B_e, cm.$^{-1}$	11.8977	14.1767
B_0, cm.$^{-1}$	11.4285	13.9318
α_e, cm.$^{-1}$	+0.9367	+0.4898
γ_e, cm.$^{-1}$	−0.0034	—
D_e, cm.$^{-1}$	0.00195	0.00141
β_e, cm.$^{-1}$	+0.00008	−0.00003
I_e, gm.-cm.^{2}*	$2.3529 \cdot 10^{-40}$	$1.9746 \cdot 10^{-40}$
r_e, cm.*	$1.2345 \cdot 10^{-8}$	$1.1310 \cdot 10^{-8}$
r_0, cm.*	$1.2596 \cdot 10^{-8}$	$1.1409 \cdot 10^{-8}$
ω_e, cm.$^{-1}$	1850.02	$\Delta G_{\frac{1}{2}} = 2739.54$
$\omega_e x_e$, cm.$^{-1}$	103.93	—
$\nu(0, 0)$, cm.$^{-1}$	23596.94	—

* *These values have been obtained from the B values with the conversion factors given by Herzberg (9).*

E. Nature of Band Emitter

The values of the rotational constants B found above from the fine structure of the new bands, if compared with the B values of other diatomic molecules, prove unambiguously that the emitter must be a neutral or ionized hydride molecule of an element between Li and F*. The fact that the bands appear in interstellar absorption (see section *F*) shows conclusively that their lower $^1\Sigma$

* *Going to extremes one might also consider SH and HCl, but they can also be eliminated in much the same way as shown below for all but one of the hydrides of Li to F.*

state must be the ground state of the molecule. The ground states of the molecules LiH, BeH, BeH^+, BH, BH^+, CH, NH, OH, OH^+, HF are known [see Table 36 in Herzberg (9)], but their B_e, B_0 and $\Delta G_{\frac{1}{2}}$ values do not agree with those observed for the lower state of the new bands. Therefore only the ionized molecules LiH^+, CH^+, NH^+, HF^+ remain to be considered as possible emitters of the new bands. However, of these four molecules only CH^+ (as it has an even number of electrons) can have singlet states. Since the new bands are definitely singlet bands we conclude that they are due to the CH^+ molecule. This conclusion appears inevitable except for the remote possibility of a doubly ionized hydride molecule as the emitter. However, this appears extremely unlikely and will be definitely excluded below.

We have purposely refrained, in the above proof, from making use of arguments based on the conditions of excitation, since in the past many wrong identifications have been made on this basis. However, it is gratifying that the identification of the emitter as CH^+ is exceedingly plausible from the point of view of the conditions of excitation. One would expect in discharges of the type described above mainly bands due to C_2 and CH and the corresponding ionized molecules, and from the singlet structure of the bands and the B values one would immediately conclude that the emitter must be CH^+ (CH and CH^{++} have no singlet states). To be sure, CN and NH bands appeared as impurities. While the new bands certainly do not belong to NH, whose spectrum is known, nor to NH^+, which would have doublet bands, NH^{++}, although exceedingly unlikely, cannot immediately be excluded on this basis (see however below).

It is well known that the r_e'' values of the neutral diatomic hydrides of each period of the periodic system form a fairly smooth curve if plotted against the atomic number [see Fig. 180 of reference (9)]. The same would be expected for the ionized hydrides. In Fig. 2, instead of the r_e'' values, the B_e'' values are plotted against the number of outer electrons since the B_e values do not involve any assumption about the atomic masses. It is seen that the B_e'' value of the new bands fits exceedingly well into the curve for the ionized hydrides if CH^+ is taken to be the emitter. This would also exclude the molecules LiH^+, NH^+, and HF^+ if they were not already excluded on the basis of the previous argument. But in addition this diagram excludes also the possibility (left open above) of a doubly ionized molecule. The B values of the doubly ionized hydrides would lie on a third curve whose approximate position is indicated by a dotted line in Fig. 2. The only doubly ionized hydride molecule that would exhibit a $^1\Pi - {}^1\Sigma$ system as a resonance transition would be NH^{++}. Even considering the uncertainty of the dotted curve in Fig. 2, it appears certain that $B(NH^{++})$ would be larger than the observed B_e'' for the new bands. In other words, NH^{++} cannot be the emitter of the bands. Indeed it would have been hard to understand an excitation of bands of a doubly ionized molecule in a discharge in which the excitation is essentially by means of metastable He atoms of 19.7 e.v. energy.

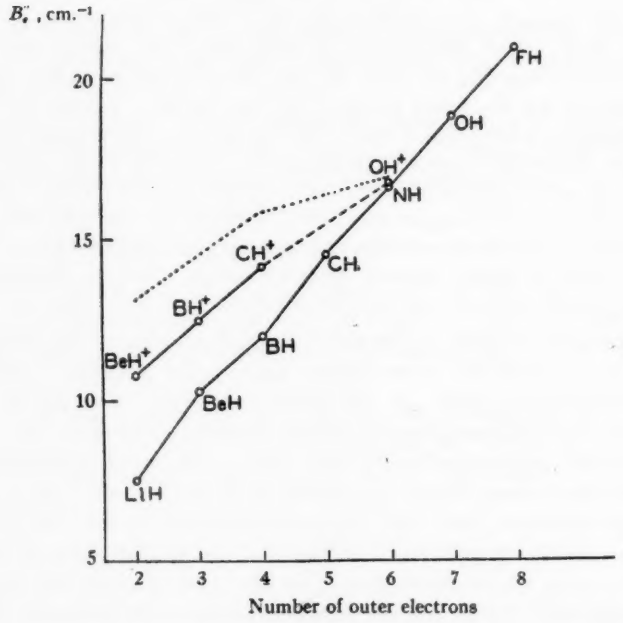

FIG. 2. *B_e'' values of neutral and ionized diatomic hydrides.*

A further proof, if such is necessary, that the new bands are due to CH^+ is the close analogy to the $^1\Pi - {}^1\Sigma^+$ bands of the BH molecule, which has the same number of electrons. The electronic excitation energy $\nu_{00} = 23596.94$ is very similar in magnitude to that of BH which is $\nu_{00} = 23073.9$. The constant q_0 of the Λ-type doubling in the $^1\Pi$ state of BH is $q_0 = 0.0337$ cm^{-1}. [see Thunberg (23)] while for CH^+ (see above) it is 0.0394. Also for both molecules $q_1 < q_0$. In both cases the q_0 values deviate in the same direction from those calculated on the assumption of pure precession [$q_0^{calc.}$ (BH) = 0.049 cm.$^{-1}$, $q_0^{calc.}$ (CH^+) = 0.044 cm.$^{-1}$, see Mulliken and Christy (19)].

Finally it is significant that the values of the internuclear distance vibrational frequency, and dissociation energy (see below) in the ground state of the emitter of the new bands ($r_e'' = 1.1310 \cdot 10^{-8}$cm., $\Delta G_{\frac{1}{2}}'' = 2739.54$, $D_0 = 3.61 \pm 0.22$ e.v.) are very close to the corresponding values of neutral CH ($r_e'' = 1.1201$, $\Delta G_{\frac{1}{2}}'' = 2732$ cm.$^{-1}$, $D_0 = 3.47 \pm 0.02$ e.v.). This is just what would be expected for CH^+ since the most loosely bound electron in CH which is removed in CH^+ is a distinctly non-bonding electron.

Recently Gerö and Schmid (7, 8) have reinvestigated certain ultraviolet bands originally discovered by McDonald (13) and have tentatively ascribed them to CH^+. Their conclusion as to the emitter of their bands appears to be far less certain than the conclusions concerning our bands. At any rate the vibrational quanta of the upper and lower states of their

bands do not agree with those of our bands. If their bands are due to CH^+ they must correspond to a transition between two fairly highly excited electronic states. Under the conditions of excitation used by us the McDonald–Gerö–Schmid bands do not occur, at least not sufficiently strongly to appear on our plates. It would be interesting to know whether our bands occur under their conditions of excitation. From the fact that they used a condensed discharge and also from the observed structure of their bands it does not appear to be impossible that their bands are due to CH^{++} (a $^2\Sigma - {}^2\Sigma$ transition would be expected for CH^{++} in about the region where these bands occur).

F. Dissociation Energy of CH^+, Ionization Potential of CH and Related Questions

The vibrational quanta of the upper state $^1\Pi$ of the CH^+ bands converge rather rapidly. A linear extrapolation gives for the dissociation energy $D_0(^1\Pi) = 7350$ cm.$^{-1}$, a value that is only twice as high above $v' = 0$ as the energy of the last observed vibrational level ($v' = 2$). According to the experience with other diatomic molecules the above value should at any rate represent an upper limit for $D_0(^1\Pi)$. On the other hand, the failure to observe bands with $v' > 2$ suggests that $v' = 2$ is the last vibrational level, or that higher levels are unstable in consequence of predissociation into another electronic state. The latter possibility can be excluded since there is only one dissociation limit in the energy range considered (see also further below). But it is entirely possible that the vibrational levels of the $^1\Pi$ state converge much faster than linearly and that in consequence of that $v' = 2$ is the last vibrational level. In this case $D_0(^1\Pi)$ would be somewhere between the last observed and the first extrapolated level ($v' = 3$), that is, equal to about 3700 cm.$^{-1}$. This value must be considered as a *lower* limit* for $D_0(^1\Pi)$. In the following we shall use the mean of the two limiting values, that is, $D_0(^1\Pi) = 5500$ cm.$^{-1}$ where the error cannot be more than ± 1800 cm.$^{-1}$. Adding $D_0(^1\Pi)$ to the electronic excitation energy 23597 cm.$^{-1}$ we obtain for the dissociation limit of the $^1\Pi$ state $E_d(^1\Pi) = 29100 \pm 1800$ cm.$^{-1} = 3.61 \pm 0.22$ e.v. above the ground state. In order to obtain from this value the dissociation energy of CH^+ we have to know the excitation energy of the products of dissociation. The lowest state of the products is $C^+(^2P) + H(^2S)$. The next two higher states are $C(^3P) + H^+(^1S)$ and $C(^1D) + H^+(^1S)$, which are 2.331 and 3.594 e.v. above the lowest state. The upper $^1\Pi$ state of the CH^+ bands cannot result from $C(^3P) + H^+(^1S)$ according to the Wigner-Witmer correlation rules ($^3P + {}^1S$ gives only triplet states). If it resulted from $C(^1D) + H^+(^1S)$ the dissociation energy of the ground state $^1\Sigma^+$ into $C^+(^2P) + H(^2S)$ would have to be $3.61 - 3.59 = 0.02 \pm 0.22$ e.v., which is im-

* *If the potential curve had a maximum it would be only an upper limit. However, even though the $^1\Pi$ state of BH has a maximum [see Herzberg and Mundie (10)] it appears very likely, on account of the much greater r_e' value, that for CH^+ a maximum, if it exists, has only a very small height.*

possible. Therefore we conclude that both states $^1\Sigma^+$ and $^1\Pi$ dissociate into $C^+(^2P) + H(^2S)$ and that the dissociation energy of CH^+ is

$$D_0(CH^+) = 3.61 \pm 0.22 \text{ e.v.}$$

From the relation

$$I(CH) + D(CH^+) = D(CH) + I(C), \qquad (3)$$

where $I(CH)$ and $I(C)$ are the ionization potentials of CH and C, respectively, one obtains, with the above value of $D(CH^+)$ and with $D(CH) = 3.47$ e.v. [see Herzberg (9)] and $I(C) = 11.267$ e.v. [see Bacher and Goudsmit (2)],

$$I(CH) = 11.13 \pm 0.22 \text{ e.v.}$$

A few years ago Smith (20) observed the appearance potential of CH^+ ions when CH_4 is bombarded with electrons of varying velocities and from it obtained two upper limits for the ionization potential of CH, $I(CH) \leqslant 11.7$ or $\leqslant 16.2$ e.v. depending on whether the mechanism for the formation of CH^+ is assumed to be $CH_4 \rightarrow CH^+ + 3H$ or $CH^+ + H_2 + H$. Later Kusch, Hustrulid, and Tate (11) from a similar study of HCN obtained an upper limit $I(CH) \leqslant 15.4$ e.v. and concluded that for CH_4 the process by which CH^+ is formed is $CH_4 \rightarrow CH^+ + H_2 + H$, since otherwise the CH^+ ions formed in the dissociation of HCN would have to have a kinetic (or vibrational) energy of at least 3.7 e.v. at the appearance potential.

Our spectroscopic value for $I(CH)$ reverses this conclusion, showing that at the appearance potential of CH^+ in HCN the products of dissociation do have an "excess" energy as high as 4.3 e.v. This result is of importance because in most discussions of the results of electron impact experiments on polyatomic molecules it has been assumed that the excess energy at the appearance potential of a certain ion is always small and certain energetically possible dissociation processes have been eliminated because they would involve fairly large "excess" energies. On the basis of the above result it is now, for example, no longer possible to exclude one of the dissociation processes $CH_4 \rightarrow CH^+ + 3H$ or $CH_4 \rightarrow CH^+ + H_2 + H$ even though the latter involves an excess energy of 5.3 e.v. at the appearance potential. It is of course not necessary to assume that all the excess energy is kinetic energy of translation. It may be also vibrational or electronic excitation energy of the products of dissociation. On the basis of the potential hyperfaces it is easy to visualize qualitatively that two competing processes may start in at one and the same energy of the bombarding electrons. It may be mentioned that even without the knowledge of the CH^+ spectrum one could have eliminated the suggested values $I(CH^+) = 16.2$ or 15.4 e.v., since on the basis of the above cycle (3) they would imply negative $D(CH^+)$ values (-1.5 and -0.7 e.v. respectively).

G. Identification of Interstellar Lines

It was mentioned in the introduction that in the case of light molecules almost exclusively the transitions from the lowest rotational level of the electronic and vibrational ground state occur in interstellar absorption.

For a $^1\Pi - {}^1\Sigma$ transition these would be the $R(0)$ lines. In Table VI the wave-lengths of the $R(0)$ lines of the 0–0, 1–0, and 2–0 CH^+ bands as observed in the laboratory, and also the observed wave-lengths of the interstellar lines, are given. The agreement is very striking, being within 0.04 Å. Even for one line the probability that it coincides by mere chance with the $R(0)$ line of a band consisting of widely spaced lines is exceedingly small. The actual agreement for all three observed bands for which an agreement is to be

TABLE VI

COMPARISON OF LABORATORY AND INTERSTELLAR WAVE-LENGTHS OF CH^+ LINES

Band	λ(Å) of $R(0)$ of CH^+ in the laboratory	Interstellar lines	Difference
0–0	4232.539	4232.58	−0.041
1–0	3957.700*	3957.72	−0.020
2–0	3745.310	3745.330	−0.020

** The $R(0)$ line of the 1–0 band is overlapped in the laboratory by the $R(5)$ line. Therefore the measured wave-length does not exactly correspond to $R(0)$. The value given here is not this directly measured wave-length but the value obtained from the band constants resulting from the other lines of the 1–0 band. It is considered to be just as reliable as the wave-lengths of the other lines.*

expected proves beyond any doubt that the interstellar lines are due to the same molecule as the new laboratory bands, that is, that they are due to the CH^+ molecule. The very small remaining difference is of the same order (0.04 Å) and in the same direction as found by McKellar (14) for CH. The difference is certainly outside the limit of accuracy of the laboratory measurements and, as pointed out by McKellar (14) and Adams (1), may possibly be due to a difference in radial velocity between interstellar Ca^+ (which is used for calibration) and interstellar CH and CH^+. While they considered a difference in the two systems of wave-lengths as also possible, the new results about CH^+ seem to make the explanation by a difference in radial velocity more likely, particularly since the line 3957.72 lies between the two Ca^+ lines (H and K).

It was at first thought that the interstellar line 3579.04 is the $R(0)$ line of the 3–0 band of CH^+. However, apart from the failure to observe this band in the laboratory there are two fairly strong reasons against this identification. (i) If the line 3579.04 is the $R(0)$ line of the 3–0 band it would be necessary to introduce a cubic term $\omega_e y_e (v + \frac{1}{2})^3$ with positive $\omega_e y_e$ into the formula for the vibrational levels (since $\Delta G'_{2\frac{1}{2}}$ would be 1242.2 cm.$^{-1}$ instead of the value 1226.44 cm.$^{-1}$ extrapolated from the ω_e' and $\omega_e x_e'$ values given in Table V). However, a positive value for $\omega_e y_e$ appears very unlikely in view of the negative value of γ_e' in Formula (2), since it is quite generally observed that the B_v and $\Delta G_{v+\frac{1}{2}}$ curves of a given electronic state have the same shape. (ii) If the value of $\omega_e' y_e'$ obtained from the identification in question is used

to extrapolate the vibrational quanta of the upper state, it is found that for no value of v' do the vibrational quanta become equal to zero.

While these arguments are not entirely cogent it would appear unlikely that the line 3579.04 is due to CH^+. Probably it is due to some other ionized molecule whose laboratory spectrum is not yet known.

It is interesting to record that Swings (21)* on the basis of our data has identified CH^+ also in the spectra of comets. In addition he has discussed in greater detail the ionization and dissociation equilibrium of CH in interstellar space.

Acknowledgments

We are greatly indebted to the American Philosophical Society for a grant from the Penrose Fund through which the grating spectrograph was provided, and to the National Research Council of Canada for a grant that made possible our collaboration.

References

1. ADAMS, W. S. Astrophys. J. 93(1) : 11-23. 1941.
2. BACHER, R. F. and GOUDSMIT, S. Atomic energy states. McGraw-Hill Book Company, Inc., New York and London. 1932.
3. BEALS, C. S. and BLANCHET, G. H. Monthly Notices Roy. Astron. Soc. 98 : 398-407. 1938.
4. DOUGLAS, A. E. and HERZBERG, G. Astrophys. J. 94 : 381. 1941.
5. DUNHAM, T., JR. Pub. Astron. Soc. Pacific, 49 : 26. 1937.
6. DUNHAM, T., JR. and ADAMS, W. S. Pub. Astron. Soc. Pacific, 49 : 5. 1937.
7. GERÖ, L. and SCHMID, R. F. Phys. Rev. (Ser. 2) 60 : 363. 1941.
8. GERÖ, L. and SCHMID, R. F. Naturwissenschaften, 29 : 504. 1941.
9. HERZBERG, G. Molecular spectra and molecular structure. I. Diatomic molecules. Prentice-Hall, Inc., New York. 1939.
10. HERZBERG, G. and MUNDIE, L. G. J. Chem. Phys. 8(3) : 263-273. 1940.
11. KUSCH, P., HUSTRULID, A., and TATE, J. T. Phys. Rev. (Ser. 2) 52(8) : 843-854. 1937.
12. LEDOUX, P. Popular Astron. 49 : 513-523. 1941.
13. MCDONALD, F. C. Abstract. Phys. Rev. (Ser. 2) 29(1): 212. 1927.
14. MCKELLAR, A. Pub. Astron. Soc. Pacific, 52 : 187-192. 1940.
15. MCKELLAR, A. Pub. Astron. Soc. Pacific, 52 : 312-318. 1940.
16. MCKELLAR, A. Dominion Astrophys. Obs., Victoria, Pub. 7(15). 1942.
17. MERRILL, P. W. Pub. Astron. Soc. Pacific, 46 : 206. 1934.
18. MERRILL, P. W. and WILSON, O. C. Astrophys. J. 87(1) : 9-23. 1938.
19. MULLIKEN, R. S. and CHRISTY, A. Phys. Rev. (Ser. 2) 38(1) : 87-119. 1931.
20. SMITH, L. G. Phys. Rev. (Ser. 2) 51(4) : 263-275. 1937.
21. SWINGS, P. Astrophys. J. 95 : 270-280. 1942.
22. SWINGS, P. and ROSENFELD, L. Astrophys. J. 86(4) : 483-486. 1937.
23. THUNBERG, S. F. Z. Physik, 100 : 471-477. 1936.

* *We wish to thank Dr. Swings for letting us see a copy of the manuscript of his paper in advance of its publication.*

THE THEORY OF SOME A-C. COMMUTATOR MOTORS WITH SERIES CHARACTERISTICS

II. THE WINTER-EICHBERG COMPENSATED REPULSION MOTOR[1]

By E. G. Cullwick[2]

Abstract

The method of analysis applied to the simple repulsion motor, in Part I of this paper (1), is now used in a study of the characteristics of the Winter–Eichberg compensated repulsion motor. Elementary explanations of this machine often contain statements that the power factor becomes leading at high speeds, but this is not necessarily true. The effect of the circulating currents in the armature coils short-circuited by the brushes may well be such that the power factor is always lagging and never reaches unity. In the development of the current locus, it is shown how this interesting effect depends on the resistance of the short-circuited coils.

1. General Theory

In the compensated repulsion motor, Fig. 1, the rotor power current I_2 is induced by transformer action, as in the simple repulsion motor, in the aa' circuit. The aa' axis, however, is made coincident with the stator axis, and the speed field ϕ_b is produced by the current I_b through a second pair of brushes bb' at right angles to aa'. The "field" current I_b may be merely the stator current I_1, but a certain flexibility is obtained if the field circuit bb' is energized from the stator circuit through a transformer of variable ratio a. With connections as shown in Fig. 1, the direction of rotation will be clockwise.

Let the positive directions of currents and fluxes be as shown. Let ϕ_a and ϕ_b be the components of the total flux linking the rotor. For the power-

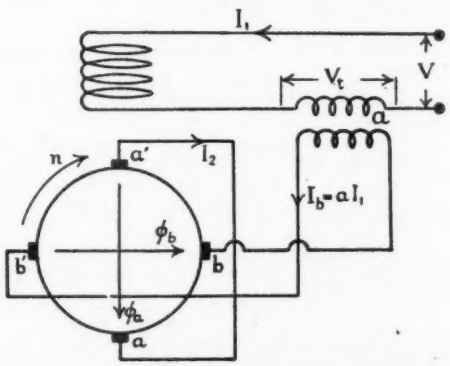

FIG. 1. *Compensated repulsion motor.*

[1] *Manuscript received in original form October 28, 1941, and as revised, February 9, 1942. Contribution from the Department of Electrical Engineering, University of Alberta, Edmonton, Alta.*

[2] *Professor and Head of Department.*

axis $a'a$, ϕ_a is the transformer field and ϕ_b the speed field. For the field axis bb', however, ϕ_a is the speed field and ϕ_b the transformer field. For the $a'a$ axis, therefore, the positive direction of the speed field (ϕ_b) lags behind the positive direction of the transformer field (ϕ_a), so that Equation (2)†* applies. Hence

$$\boldsymbol{E}_{aa'} = Q_2(-n\boldsymbol{\phi}_b + jn_s\boldsymbol{\phi}_a) = -\frac{n}{n_s}\boldsymbol{I}_bX_b + j(\boldsymbol{I}_1X_{12} - \boldsymbol{I}_2X_a), \quad (1)$$

where X_a is the rotor reactance between aa', and X_b is the reactance between bb'. Putting $\boldsymbol{I}_b = a\boldsymbol{I}_1$ and equating $\boldsymbol{E}_{aa'}$ to the resistance drop $\boldsymbol{I}_2R_a$ in the aa' circuit gives

$$\boldsymbol{I}_2 = \frac{\boldsymbol{I}_1}{Z_a^2}\left\{X_{12}(X_a + jR_a) - \frac{an}{n_s}X_b(R_a - jX_a)\right\}. \quad (2)$$

Considerable simplification will ensue if it may be assumed that $X_a \doteq X_b = X_2$ and $R_a \doteq R_b = R_2$. For the $b'b$ axis the positive direction of the speed field (ϕ_a) is in advance of the positive direction of the transformer field (ϕ_b), so that Equation (1)† applies. Hence:

$$\boldsymbol{E}_{bb'} = Q_2(n\boldsymbol{\phi}_a + jn_s\boldsymbol{\phi}_b) = \frac{n}{n_s}(\boldsymbol{I}_1X_{12} - \boldsymbol{I}_2X_2) + j\boldsymbol{I}_bX_2. \quad (3)$$

The p.d. across the brushes is

$$\boldsymbol{V}_{b'b} = \boldsymbol{E}_{bb'} + \boldsymbol{I}_bR_2, \quad (4)$$

and the p.d. across the primary of the transformer is $\boldsymbol{V}_t = a\boldsymbol{V}_{b'b}$, which from Equations (2), (3), and (4) becomes

$$\boldsymbol{V}_t = \boldsymbol{I}_1\left\{\left[a^2R_2 + a\frac{n}{n_s}\left\{X_{12} - \left(\frac{X_2}{Z_2}\right)^2X_{12}\right\} + a^2\left(\frac{n}{n_s}\right)^2\left(\frac{X_2}{Z_2}\right)^2R_2\right]\right.$$
$$\left. + j\left[a^2X_2 - a\frac{n}{n_s}\frac{X_2X_{12}}{Z_2^2}R_2 - a^2\left(\frac{n}{n_s}\right)^2\left(\frac{X_2}{Z_2}\right)^2X_2\right]\right\}. \quad (5)$$

Further, the p.d. across the stator winding is

$$\boldsymbol{V}_s = \boldsymbol{I}_1(R_1 + jX_1) - j\boldsymbol{I}_2X_{12}$$
$$= \boldsymbol{I}_1\left\{\left[R_1 + \left(\frac{X_{12}}{Z_2}\right)^2R_2 + a\frac{n}{n_s}\left(\frac{X_2}{Z_2}\right)^2X_{12}\right]\right.$$
$$\left. + j\left[X_1 - \left(\frac{X_{12}}{Z_2}\right)^2X_2 + a\frac{n}{n_s}\frac{X_{12}X_2}{Z_2^2}R_2\right]\right\}. \quad (6)$$

The motor terminal p.d. is then $\boldsymbol{V} = \boldsymbol{V}_t + \boldsymbol{V}_s = \boldsymbol{I}_1\boldsymbol{Z}_{st}$, where

$$\boldsymbol{Z}_{st} = \left\{R_1 + a^2R_2 + R_2\left(\frac{X_{12}}{Z_2}\right)^2\right\} + j\left\{X_1 + a^2X_2 - X_2\left(\frac{X_{12}}{Z_2}\right)^2\right\}$$
$$+ a\frac{n}{n_s}\left\{X_{12} + a\frac{n}{n_s}R_2\left(\frac{X_2}{Z_2}\right)^2 - ja\frac{n}{n_s}X_2\left(\frac{X_2}{Z_2}\right)^2\right\}. \quad (7)$$

The term a^2X_2 is the reactance of the "field winding" bb', and at synchronous speed is roughly compensated by the last term in Equation (7),

* *In this paper, a dagger (†) following an equation number indicates that the equation is the one bearing that number in Part I of this series (1).*

which gives the rotational e.m.f. per ampere induced between bb' by the "transformer flux" ϕ_a ; hence the name "compensated" repulsion motor.* The vector diagram is shown in Fig. 2.

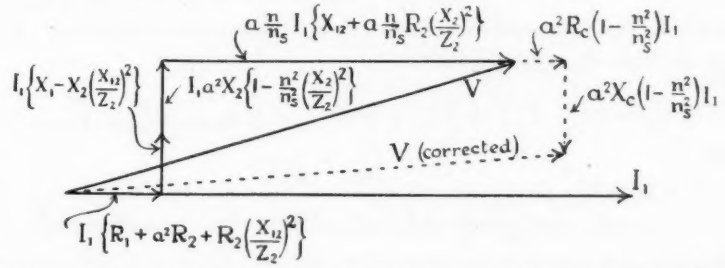

FIG. 2. *Compensated repulsion motor. Vector diagram. Dotted lines show the effect of the short-circuited coils.*

From Equation (7) it is found that the power factor is unity when

$$\left(\frac{n}{n_s}\right)^2 = \frac{X_1 + a^2X_2 - X_2(X_{12}/Z_2)^2}{a^2X_2(X_2/Z_2)^2} . \tag{8}$$

The copper loss is $P_c = I_1^2R_1 + (a^2I_1^2 + I_2^2)R_2$, whence, from Equation (2),

$$\frac{P_c}{I_1^2} = R_1 + a^2R_2 + R_2\left\{\left(\frac{X_{12}}{Z_2}\right)^2 + a^2\frac{n^2}{n_s^2}\left(\frac{X_2}{Z_2}\right)^2\right\} . \tag{9}$$

The gross motor power is equal to the input less the copper loss, or

$$P_m = I_1^2a\frac{n}{n_s}X_{12} . \tag{10}$$

The gross torque

$$T = 0.117\frac{P_m}{n}, \tag{10a}$$

---

* *If* $\mathbf{Z}_a \neq \mathbf{Z}_b$, *Equations (5), (6), (7) become:*

$$\mathbf{V}_1/\mathbf{I}_1 = \left\{a^2R_b + a\frac{n}{n_s}X_{12}\left(1 - \frac{X_a^2}{Z_a^2}\right) + a^2\left(\frac{n}{n_s}\right)^2\frac{X_aX_b}{Z_a^2}R_a\right\} + j\left\{a^2X_b - a\frac{n}{n_s}\frac{X_aX_{12}}{Z_a^2}R_a - a^2\left(\frac{n}{n_s}\right)^2\frac{X_a^2}{Z_a^2}X_b\right\}, \tag{5a}$$

$$\mathbf{V}_a/\mathbf{I}_1 = \left\{R_1 + \left(\frac{X_{12}}{Z_a}\right)^2R_a + a\frac{n}{n_s}\frac{X_aX_b}{Z_a^2}X_{12}\right\} + j\left\{X_1 - \left(\frac{X_{12}}{Z_a}\right)^2X_a + a\frac{n}{n_s}\frac{X_{12}X_b}{Z_a^2}R_a\right\}, \tag{6a}$$

and

$$\mathbf{Z}_{at} = \left\{R_1 + a^2R_b + R_a\left(\frac{X_{12}}{Z_a}\right)^2\right\} + j\left\{X_1 + a^2X_b - X_a\left(\frac{X_{12}}{Z_a}\right)^2\right\} + a\frac{n}{n_s}\left[\left\{X_{12} - \frac{X_aX_{12}}{Z_a^2}(X_a - X_b) + a\frac{n}{n_s}\frac{X_aX_b}{Z_a^2}R_a\right\} - j\left\{\frac{R_aX_{12}}{Z_a^2}(X_a - X_b) + a\frac{n}{n_s}\left(\frac{X_a}{Z_a}\right)^2X_b\right\}\right] . \tag{7a}$$

If Equation (7a) is made the basis of the construction of the current locus in Fig. 3, the chief difference will be that the line RS will deviate slightly to the left of the vertical.

which is seen to be a function of the current only, as in other series motors. In terms of V and n

$$T = 0.117 \frac{aV^2}{n_s Z_a^2}, \tag{11}$$

which is a very complicated expression unless resistances are neglected. If this is done we have the approximation:

$$Z_a^2 \doteq \left(a\frac{n}{n_s}X_{12}\right)^2 + \left(X_1 + a^2X_2 - X_{12}^2/X_2 - a^2\frac{n^2}{n_s^2}X_2\right)^2, \tag{12}$$

so that

$$T \doteq 0.117 \frac{V^2}{n_s} \frac{aX_{12}}{\left(a\frac{n}{n_s}X_{12}\right)^2 + \left(X_1 + a^2X_2 - X_{12}^2/X_2 - a^2\frac{n^2}{n_s^2}X_2\right)^2}. \tag{13}$$

The starting torque

Putting $n = 0$ in Equation (13) we have, neglecting resistances,

$$T_S \doteq 0.117 \frac{V^2}{n_s} \frac{aX_{12}}{[X_1 + X_2\{a^2 - (X_{12}/X_2)^2\}]^2}. \tag{14}$$

Differentiating Equation (14) with respect to a, we find for the maximum starting torque for a given terminal p.d.:

$$a^2 = \frac{X_1X_2 - X_{12}^2}{3X_2^2}. \tag{15}$$

Example: If $X_1 = 51.5$, $X_2 = 6.57$, $X_{12} = 17.4$, the maximum starting torque with full-voltage starting is when $a = 0.525$.

2. Rough Approximations

If we neglect both resistance and leakage reactance, and assume that the winding coefficients are identical, we may put as before: $X_1 = cN_1^2$, $X_2 = cN_2^2$, $X_{12} = cN_1N_2$, whence

$$Z_{et} \doteq a\frac{n}{n_s}X_{12} + ja^2X_2(1 - n^2/n_s^2). \tag{16}$$

Thus, in the "ideal" motor, the power factor is unity at synchronous speed, and this relation is independent of the transformer ratio a.

The power factor angle θ is given approximately by

$$\tan\theta \doteq a\frac{N_2}{N_1}\left(\frac{n_s^2 - n^2}{n_s n}\right), \tag{17}$$

so that the power factor can be improved at speeds above and below synchronism by reducing the ratio a by tap-changing on the transformer.

The power factor, neglecting resistance, but allowing for leakage. Let $N_1/N_2 = b$, and $x_s = x_1 + b^2x_2$ the equivalent leakage reactance of the motor, x_1 being the sum of the leakage reactances of stator and transformer referred to

the primary. Then, from Equation (6*a*)†: $X_1X_2 - X_{12}^2 = X_{12}\frac{x_e}{b}$. Neglecting resistance we have from Equation (7):

$$\tan\theta = \frac{X_1X_2 - X_{12}^2 + a^2X_2^2(1 - n^2/n_s^2)}{a\frac{n}{n_s}X_2X_{12}}$$

$$= \frac{n_s}{n}\cdot\frac{x_e}{abX_2} + a\frac{X_2}{X_{12}}\left(\frac{n_s^2 - n^2}{n_s n}\right), \tag{18}$$

so that at synchronous speed:

$$\tan\theta \doteq \frac{x_e}{abX_2}. \tag{19}$$

3. Commutation in the Compensated Repulsion Motor

Referring to Fig. 1, we shall take the positive direction of the e.m.f's induced in the coils short-circuited by aa' as that which would cause a current having an m.m.f. from b to b': i.e., opposed to the positive direction of ϕ_b. Similarly, we shall take the positive direction of the e.m.f's induced in the coils short-circuited by bb' as that which would cause a current having an m.m.f. opposed to the direction of ϕ_a.

Commutation at aa'. For the coil short-circuited by aa', ϕ_b is the transformer field and ϕ_a the speed field. Since ϕ_a is in advance of ϕ_b it follows that Equation (1)† applies. Hence the e.m.f. induced in the shorted coil is

$$\boldsymbol{E}_a = Q_s(n\boldsymbol{\phi}_a + jn_s\boldsymbol{\phi}_b).$$

From Equation (1):

$$\boldsymbol{\phi}_a = \frac{\boldsymbol{I}_1X_{12} - \boldsymbol{I}_2X_2}{Q_2n_s}.$$

If resistances are neglected, this becomes, from Equation (2):

$$\boldsymbol{\phi}_a = -j\boldsymbol{I}_1\frac{X_2an}{Q_2n_s^2}, \tag{20}$$

and

$$\boldsymbol{\phi}_b = a\frac{\boldsymbol{I}_1X_2}{Q_2n_s}. \tag{21}$$

Let

$$\frac{Q_s}{Q_2}X_2 = X_{rm} \doteq \tfrac{1}{2}\pi\frac{N_s}{N_2}X_2, \tag{22}$$

the mutual reactance between the shorted coil and the rest of the rotor winding. Then

$$\boldsymbol{E}_a = ja\boldsymbol{I}_1X_{rm}\{1 - (n/n_s)^2\}, \tag{23}$$

and we see that the commutation at aa' is inherently good only at synchronous speed.

To find $\boldsymbol{E}_a$ at starting, neglecting resistance and leakage we have

$$a\boldsymbol{I}_1 = \frac{a\boldsymbol{V}}{\boldsymbol{Z}_{st}} \doteq \frac{\boldsymbol{V}}{jaX_2},$$

from Equation (16), so that

$$\boldsymbol{E}_{a_{(n=0)}} \doteq \frac{X_{sm}}{X_2}\frac{\boldsymbol{V}}{a}. \tag{24}$$

Thus the commutation at aa' can be improved at starting by increasing a. This, however, is at the expense of the starting torque (Equation (15)).

Commutation at bb'. For the coil short-circuited by bb', ϕ_a is the transformer field and ϕ_b is the speed field. Since ϕ_b lags behind ϕ_a, Equation (2)† applies. Hence the e.m.f. induced in the shorted coil is

$$E_b = Q_s(-n\phi_b + jn_s\phi_a);$$

from Equations (20) and (21) this becomes

$$E_b \doteq aI_1X_{rm}\left(\frac{n}{n_s} - \frac{n}{n_s}\right) = 0 \tag{25}$$

Thus the inherent commutation at the excitation brushes bb' is good at all speeds, the only appreciable e.m.f. in the short-circuited coils being the usual "reactance voltage" caused by the current reversal.

4. The Effect of the Short-circuited Coils on the Performance of the Compensated Repulsion Motor

From Equation (25) it is seen that the effect of the currents in the coils short-circuited by bb' will be negligible. We shall confine our attention to the coils shorted by the power brushes aa'.

The short-circuit current in these coils is

$$I_s = \frac{E_a}{R_s + jX_s} = jaI_1\frac{X_{rm}}{Z_s^2}(R_s - jX_s)\{1 - (n/n_s)^2\} \tag{26}$$

in a direction opposed magnetically to ϕ_b. This current induces a transformer e.m.f. from b to b' given by

$$E_{bs} = -jI_sX_{sm} = aI_1\left(\frac{X_{rm}}{Z_s}\right)^2(R_s - jX_s)\{1 - (n/n_s)^2\}, \tag{27}$$

and a rotational e.m.f. between a and a' which is zero at both standstill and synchronism,* and which as in the case of the simple repulsion motor will be neglected. The terminal p.d. of the motor must therefore be increased by an amount equal to aE_{bs}, so that the equivalent impedance of the motor is increased by

$$Z' = a^2\frac{X_{rm}^2}{Z_s}(R_s - jX_s)\{1 - (n/n_s)^2\}, \tag{28}$$

which should be compared with Equations (33)† and (34)† for the simple repulsion motor. Putting

$$\left(\frac{X_{rm}}{Z_s}\right)^2R_s = R_c, \quad \text{and} \quad \left(\frac{X_{rm}}{Z_s}\right)^2X_s = X_c \tag{29}$$

we have

$$Z' = a^2(R_c - jX_c)\{1 - (n/n_s)^2\}. \tag{30}$$

The effect on the vector diagram is shown by the dotted lines in Fig. 2

* *See note at end of Part I of this series (1).*

The *copper loss* in the short-circuited coil is, as in the case of the simple repulsion motor (Equation (35)†),

$$I_s^2 R_s = \frac{E_a^2}{Z_s^2} R_s = I_1^2 a^2 R_c \left(1 - \frac{n^2}{n_s^2}\right)^2 \tag{31}$$

and since the input is increased by $I_1^2 a^2 R_c \left(1 - \frac{n^2}{n_s^2}\right)$, the *gross power* is increased by

$$P_{mc} = I_1^2 a^2 R_c \frac{n^2}{n_s^2}\left(1 - \frac{n^2}{n_s^2}\right) \tag{32}$$

while the *gross torque* is increased by

$$T_c = 0.117 \frac{P_{mc}}{n} \tag{33}$$

exactly as in the case of the simple repulsion motor.

We then have:

The equivalent standstill resistance

$$R_s' = R_1 + a^2 R_2 + R_2 \left(\frac{X_{12}}{Z_2}\right)^2 + a^2 R_c . \tag{34}$$

The equivalent standstill reactance

$$X_s' = X_1 + a^2 X_2 - X_2 \left(\frac{X_{12}}{Z_2}\right)^2 - a^2 X_c . \tag{35}$$

The rotational e.m.f.

$$E_r' = - I_1 a \frac{n}{n_s}\left[X_{12} - a \frac{n}{n_s}\left\{R_2 \left(\frac{X_2}{Z_2}\right)^2 - R_c - j\left[X_2 \left(\frac{X_2}{Z_2}\right)^2 - X_c\right]\right\}\right]. \tag{36}$$

The copper loss is given by

$$\frac{P_c'}{I_1^2} = \frac{P_c}{I_1^2} + a^2 R_c \left(1 - \frac{n^2}{n_s^2}\right)^2, \text{ where } P_c/I_1^2 \text{ is given by Equation (9).} \tag{37}$$

The gross motor power

$$P_m' = I_1^2 a \frac{n}{n_s}\left\{X_{12} + a R_c \frac{n}{n_s}\left(1 - \frac{n^2}{n_s^2}\right)\right\}. \tag{38}$$

The gross torque

$$T' = 0.117 \frac{P_m'}{n} . \tag{38a}$$

The total equivalent impedance

$$\begin{aligned} \boldsymbol{Z}_{st}' = {} & \left\{R_1 + a^2 R_2 + R_2 \left(\frac{X_{12}}{Z_2}\right)^2 + a^2 R_c\right\} + j\left\{X_1 + a^2 X_2 - X_2 \left(\frac{X_{12}}{Z_2}\right)^2 - a^2 X_c\right\} \\ & + a \frac{n}{n_s}\left\{X_{12} + a \frac{n}{n_s}\left[R_2 \left(\frac{X_2}{Z_2}\right)^2 - R_c\right] - ja \frac{n}{n_s}\left[X_2 \left(\frac{X_2}{Z_2}\right)^2 - X_c\right]\right\}, \end{aligned} \tag{39}$$

which can easily be rearranged in the form $\boldsymbol{Z}_{st}' = R_{st}' + jX_{st}'$.

5. The Current Locus for Constant Reactances

(*a*) *No correction for short-circuit currents*

In Fig. (3):

$$OX = X_1 + a^2X_2 - X_2\left(\frac{X_{12}}{Z_2}\right)^2$$

$$XR = R_1 + a^2R_2 + R_2\left(\frac{X_{12}}{Z_2}\right)^2$$

$$RS = \frac{n}{n_s}X_{12}, \qquad SN = \left(a\frac{nX_2}{n_sZ_2}\right)^2, \quad \tan y = \frac{R_2}{X_2}.$$

Then ON is the reflected impedance vector when short-circuit currents are neglected, and the locus of N is clearly a parabola, the inverse of which, with respect to O, is the current locus. The limits of *power factor* are:

Standstill $\tan \theta_s = OX/XR$, lagging,
Infinite speed $\tan \theta_\infty = X_2/R_2$, leading.

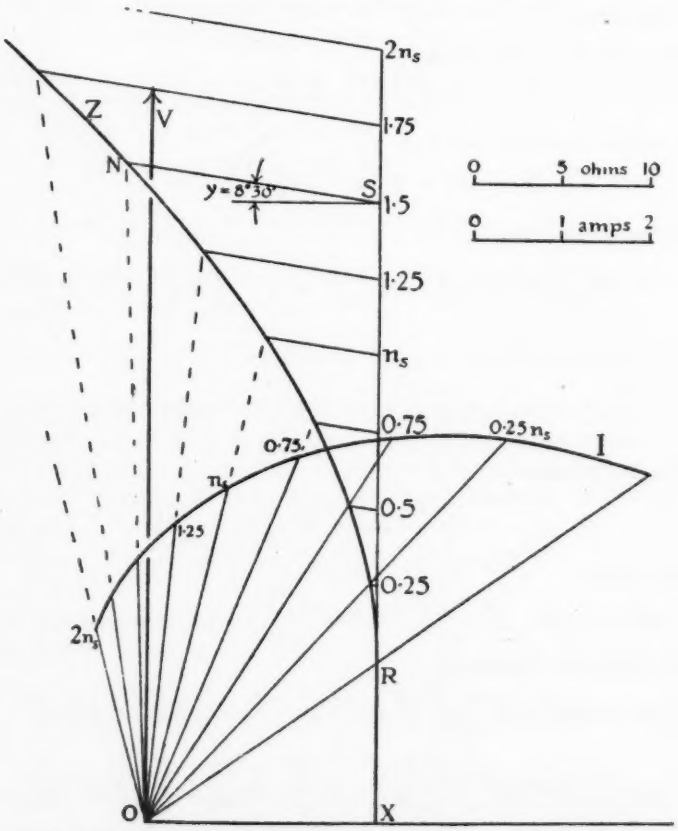

FIG. 3. *Compensated repulsion motor. Case (a), no correction.*

(*b*) *Including the effect of the short-circuited coils*

This is shown in Fig. 4, in which:

$$OX' = OX - a^2X_c, \quad X'R' = XR + a^2R_c, \quad R'S' = a\frac{n}{n_s}X_{12},$$

$$S'N' = a^2\frac{n^2}{n_s^2}\sqrt{R_r^2 + X_r^2}, \text{ where } R_r = R_2\left(\frac{X_2}{Z_2}\right)^2 - R_c$$

$$\text{and } X_r = X_2\left(\frac{X_2}{Z_2}\right)^2 - X_c.$$

$$\tan y' = R_r/X_r.$$

The locus of the impedance vector is then $R'N'$, which crosses the locus RN of Fig. 3 at synchronous speed.

The sign of X_r depends on the value of R_s. If both R_2 and R_s are zero, we have in the "ideal motor", from Equations (29) and (22) and Equation (31)†:

$$X_c \doteq \frac{X_m^2}{X_s} \doteq \frac{\pi}{2}X_2, \qquad \text{and} \qquad X_r = -\left(\frac{\pi}{2} - 1\right)X_2,$$

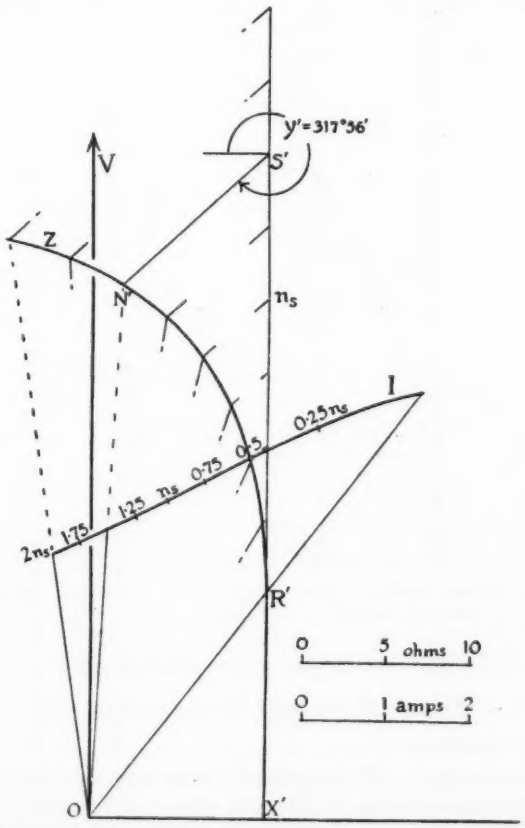

FIG. 4. *Compensated repulsion motor. Case (b), $R_s = 0.5$.*

in which case the locus $R'N'$ curves to the right and the power factor never becomes unity.

There are three possible cases according to the relative magnitudes of $X_2(X_2/Z_2)^2$ and X_c :

(*A*) $X_c < X_2(X_2/Z_2)^2$. The impedance locus $R'N'$ is a parabola curving to the left as in Fig. 4, and the power factor passes through unity and becomes leading at high speeds.

(*B*) $X_c = X_2(X_2/Z_2)^2$. The impedance locus is a vertical straight line as shown in Fig. 5, and the current locus is a circle. Further, if

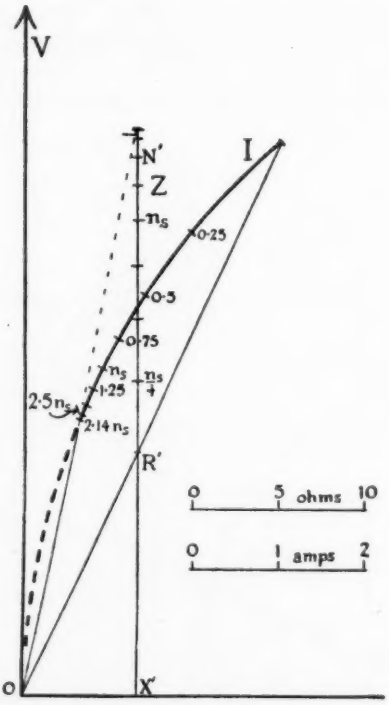

FIG. 5. *Compensated repulsion motor. Case (c), R_e = 0.224. Maximum P.F. = 0.980 at 2.14 n_s. Minimum current = 3.28 amp.*

$R_e < R_2(X_2/Z_2)^2$, the power factor reaches unity at infinite speed, but if $R_e > R_2(X_2/Z_2)^2$ the power factor increases until $n = \frac{X_{12}}{2aR_r} n_s$, and then decreases.

(*C*) $X_c > X_2(X_2/Z_2)^2$. The impedance locus is a parabola curving to the right, as shown in Fig. 6., and the power factor rises to a maximum value (lagging) at some finite speed and never becomes leading.

Example. As an example, suppose the previous figures* refer to a compensated repulsion motor, for which $a = 1$. Then: $X_2 = 6.57$, $X_2(X_2/Z_2)^2 = 6.42$, $X_s = 0.286$, $X_{rm} = \frac{6.57\pi}{6 \times 2} = 1.719$, $R_2 = 0.98$. Table I gives the data for the construction of the current locus for each of the two cases: (*a*) No

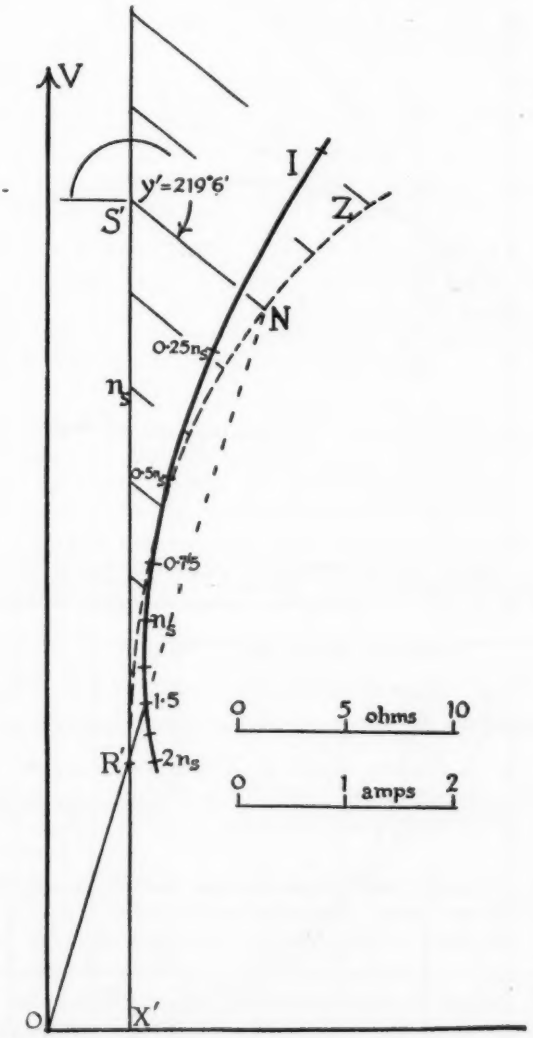

FIG. 6. *Compensated repulsion motor. Case (d), $R_s = 0.1$. Maximum P.F. = 0.976 at $n = 0.55\, n_s$.*

* *Part I of this series (1).*

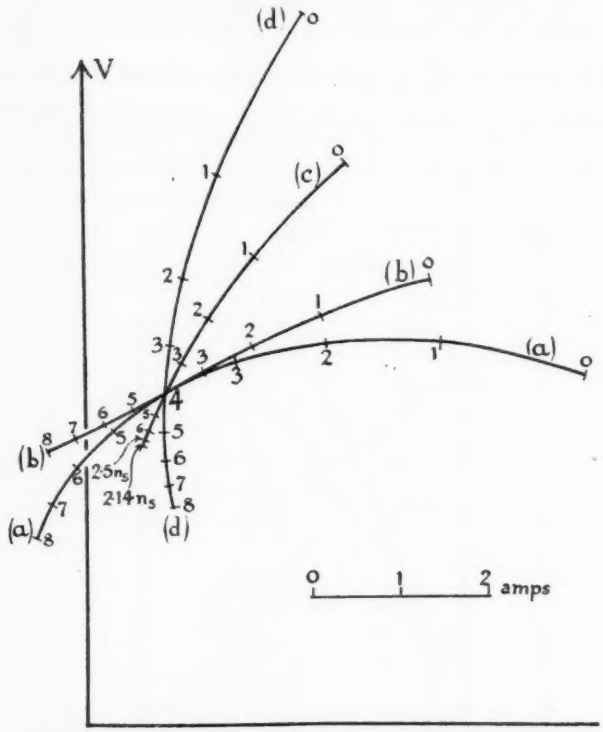

FIG. 7. *Compensated repulsion motor. Current loci. (a) No correction, (b) $R_s = 0.5$, (c) $R_s = 0.224$, (d) $R_s = 0.1$. Figures denote quarters of synchronous speed.*

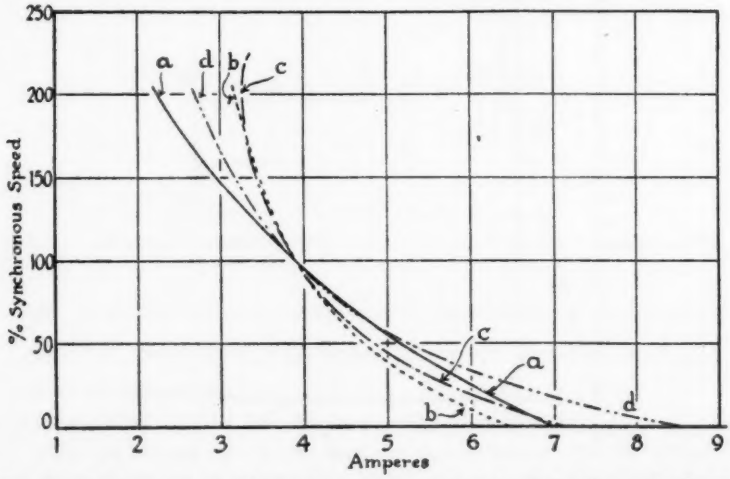

FIG. 8. *Compensated repulsion motor. Effect of short-circuited coils on speed-current curves.*

correction for short-circuit currents, Fig. 3; (*b*) $R_s = 0.5$, Fig. 4; (*c*) $R_s = 0.224$, Fig. 5; and (*d*) $R_s = 0.1$, Fig. 6.

TABLE I

DATA FOR FIGS. 3, 4, 5, AND 6

	OX	XR	RS			SN	y
(*a*) No correction Fig. 3	13.0	9.08	$17.4\frac{n}{n_s}$			$6.5\left(\frac{n}{n_s}\right)^2$	8°30′
	OX'	$X'R'$	$R'S'$	R_r	X_r	$S'N'$	y'
(*b*) $R_s = 0.5$ Fig. 4	10.45	13.53	$17.4\frac{n}{n_s}$	−3.49	3.87	$5.21\left(\frac{n}{n_s}\right)^2$	317°56′
(*c*) $R_s = 0.224$ Fig. 5*	6.58	14.10	$17.4\frac{n}{n_s}$	−4.06	0	$4.06\left(\frac{n}{n_s}\right)^2$	270°
(*d*) $R_s = 0.1$ Fig. 6	3.8	12.3	$17.4\frac{n}{n_s}$	−2.26	−2.78	$3.58\left(\frac{n}{n_s}\right)^2$	219°6′

* *That is,* $R'N' = 17.4\frac{n}{n_s} - 4.06\left(\frac{n}{n_s}\right)^2$, *and is vertical.*

The current loci for the four cases are shown superimposed in Fig. 7 in which it is seen that they all intersect at synchronous speed. The figures 1, 2, 3, . . . shown along the loci denote quarters of synchronous speed. Current-speed curves for the four cases are shown in Fig. 8.

In these diagrams the speed has been extended above the theoretical no-load speed, at which the gross torque (Equation (38*a*)) becomes zero. It differs slightly in the three cases, but is in the neighbourhood of $1.75\,n_s$.

6. The Effect of Saturation

If resistances and leakage reactance are neglected, it is found that

$$\boldsymbol{\phi}_b = Ka\boldsymbol{I}_1N_2, \quad \text{and} \quad \boldsymbol{\phi}_a = -jKa\boldsymbol{I}_1N_2\frac{n}{n_s} = -j\boldsymbol{\phi}_a\frac{n}{n_s},$$

so that at synchronous speed the windings produce a "rotating" m.m.f. of constant amplitude proportional to aI_1N_2. Hence the values of the reactances, neglecting the variation due to departure from synchronous speed, should be found as follows:

(1) Given curves showing X_1 and X_{12} as functions of I_1, the values of X_{12} and X_1 for a given stator current I_1 under operating conditions are those corresponding to a current equal to $aI_1N_2/N_1 = aX_{12}I_1/X_1$ on the X_1 and X_{12} graphs.

(2) The value of X_2 is that corresponding to a current $I_b = aI_1$ on the X_2/I_b curve.

References

1. CULLWICK, E. G. Can. J. Research, A, 20 : 49-70. 1942.
2. FORD, W. Elec. Rev. 103 : 595-598. 1928.

Canadian Journal of Research

Issued by THE NATIONAL RESEARCH COUNCIL OF CANADA

VOL. 20, SEC. B. JUNE, 1942 NUMBER 6

THE REMOVAL OF COPPER AND CADMIUM IN THE HYDROMETALLURGY OF ZINC[1]

BY G. T. E. GRAHAM[2] AND T. THORVALDSON[3]

Abstract

A study was made of the precipitation, by means of zinc dust, of copper and cadmium from a "normal thickener overflow" solution as obtained in the hydrometallurgy of zinc. The effect of (i) the quantity of zinc dust added, (ii) the initial pH of the solution, (iii) the time of agitation, and (iv) the aeration of the solution were studied. The polarograph was used to follow the changes in the concentration of the solution.

For the effective removal of cadmium, the initial pH of the solution should not be below 3.5. The time of treatment with zinc dust should be controlled within narrow limits and, while the agitation should be effective, it should not cause aeration of the solution. The redissolving of cadmium on prolonged treatment appears to be a typical process of electrolytic corrosion analogous to underwater corrosion of iron in the neutral zone, the rate of redissolving being dependent on the supply of oxygen for depolarization. Similar redissolving of copper does not take place under the conditions studied and, given sufficient zinc dust, only the minimum time of treatment need be controlled.

In the hydrometallurgy of zinc as carried out at the Flin Flon Plant of the Hudson Bay Mining and Smelting Company (1), there is obtained a solution (called "neutral thickener overflow") containing zinc sulphate in high concentration with small quantities of other metals as impurities. A typical assay of this solution gives the following values in grams per litre: Zn, 120; Cu, 0.221; Cd, 0.152; Mn, 0.049; Fe, 0.031; Co, 0.012; As, 0.0008; Mg, 17.6; Ca, 2.52; suspended solids, 1.0. It is essential to remove the major portion of the copper and cadmium present in this solution before it can be electrolyzed to produce zinc of high purity. This is effected by agitation of the liquid with zinc dust in a batch or continuous process until the amounts of copper and cadmium in solution have been reduced to within the permissible limits. The object of this study was to determine the effect of such factors as the proportion of zinc dust used, the time of agitation, and the hydrogen ion concentration (pH) of the solution on the removal of copper and cadmium from the neutral thickener overflow.

[1] *Manuscript received March 2, 1942.*

Contribution from the Department of Chemistry, University of Saskatchewan, Saskatoon, Sask.

[2] *Graduate Student, University of Saskatchewan; at the time, the holder of a Bursary under the National Research Council of Canada.*

[3] *Professor of Chemistry and Lecturer in Metallurgy.*

Materials and Experimental Procedure

The neutral thickener overflow (N.T.O.) solution and the zinc dust used were supplied by the Hudson Bay Mining and Smelting Company from their Zinc Plant at Flin Flon. In order to ensure an approximately constant ratio of surface to weight of zinc in different series of experiments, the zinc dust was sieved and the 140 to 200 mesh fraction used (A.S.T.M. Standard). The solution, which for most of the work was of the composition given above, was filtered to remove suspended solids.

The solution which, unless otherwise stated, had an initial pH value of 5.27 was treated with zinc dust in a cylindrical glass jar in two-litre batches and stirred by means of an efficient motor driven glass stirrer. All the experiments were carried out in a thermostat at 40.0° C. ± 0.1°, this temperature being chosen so as to conform to plant conditions at Flin Flon. Samples of the liquid for analysis were removed by means of a 100 ml. pipette, the tip of which was fitted with a glass wool filter. This effected complete and rapid separation of the liquid from the suspended solids. All pH measurements were made at 21° C. with a Leeds and Northrup Universal pH Indicator, using a glass electrode. The results were reproducible within a pH of ±0.02.

The Determination of Copper and Cadmium

The selection of a suitable method for the rapid and accurate determination of copper and cadmium in the N.T.O. solution before and after the treatment with zinc dust presented some difficulty. A suitable method must be capable of the accurate determination of these substances in concentrations varying from that originally present in the N.T.O. (220 mg. of copper per litre and 150 mg. of cadium per litre) down to about one milligram per litre in presence of 120 gm. of zinc per litre. A number of methods, electrolytic and colorimetric, were studied and found unsatisfactory before it was decided to use the polarographic method.

This method, originally developed by Heyrovsky (2) and applied to quantitative determinations by him and his co-workers at the Charles University in Prague, is based on the interpretation of current-voltage curves obtained by electrolyzing the unknown solution in a cell with a capillary mercury dropping electrode (tip of about 0.03 mm. inside diameter), dropping at a rate of one drop every two to four seconds, and a stationary pool of mercury as the other electrode. Each electro-reducible substance in the solution produces its own characteristic "wave" on the curve, so that under the optimum conditions it is possible to detect and determine both the species and concentration of several such substances in a solution from a single current-voltage curve. The method is especially suitable for the concentrations of from 10^{-6} to 10^{-2} molar, the attainable accuracy being within about 2% when the concentration is greater than 10^{-4} and within 10% when it is between 10^{-4} and 10^{-5} molar. For a detailed discussion of the method and its applications, the reader is referred to a paper by Kolthoff and Lingane (3).

The Polarographic Equipment

Only a few of the essential details of the equipment will be given. The electrolytic cell was of Pyrex glass, of 55 ml. capacity, and was designed so as to facilitate the introduction and removal of the test solution by means of a side-tube without disturbing the dropping electrode. A saturated calomel reference electrode was attached by means of a ground glass joint to a side-tube of the cell, the saturated potassium chloride and the test solution being separated by a porous ground-glass plug. A stream of nitrogen purified by alkaline pyrogallol, which was introduced into the cell near the bottom, was used to remove all oxygen from the test solution before the electrolysis. A trap was provided for the escape of the nitrogen from the cell.

The variable potential was obtained from a battery by using two potentiometer-type rheostats connected in series, one of 1000 ohms resistance for coarse adjustment and one of 10 ohms for fine adjustment. The galvanometer, which was critically damped, had a sensitivity of 0.0023 micro amperes per millimetre scale division and its shunt consisted of a precision resistance box. A Leeds and Northrup student type potentiometer and Weston standard cell for calibration were also used. A dial-type double pole switch was installed so that the following potentiometric measurements could be readily made.

1. Potential drop across the resistance box for calculating the current as a check on the galvanometer measurements.
2. The total applied potential between the dropping electrode and the stationary mercury pool.
3. The potential of the dropping electrode against the calomel reference electrode.
4. The potential of the quiet mercury pool against the calomel electrode.

At the beginning of each run the dropping time was adjusted to 3.00 sec. by means of a system of levelling bulbs. When great pains were taken in the purification of the mercury, the dropping electrode worked well during several months of use. When it began to show erratic behaviour it was found preferable to make and recalibrate a new one rather than try to clean the tip.

The polarographic measurements were made at 21° C. The temperature of the room itself fluctuated only slightly from this temperature.

Calibration of the Polarograph

The polarograph was calibrated with a series of solutions of known concentration of which the copper content varied from 5 to 250 mg. per litre, and the cadmium from 5 to 150 mg. per litre, whereas the concentration of zinc remained constant at 120 gm. per litre, all present as the sulphates. In order to eliminate maxima on the current-voltage curves, 10 drops (0.30 ml.) of a 0.2% methyl red solution was added in each case to 55 ml. of the test

solution, and a resistance of 9000 ohms was used in series with the cell. For solutions containing copper and cadmium in the higher concentrations, a shunt of 9 ohms was used with the galvanometer, whereas for the lower concentrations this was changed to a shunt of 150 ohms to increase the height of the wave and the accuracy of the wave height determination. Fig. 1 gives an example of a current-voltage curve for a solution containing 150 mg. of copper per litre, 125 mg. of cadmium per litre, and 120 gm. of zinc per litre, using a 9 ohm shunt. The half-wave potential for copper under the conditions of the experiments was found to be -0.02 volts and for cadmium, -0.61 volts, with respect to the saturated calomel electrode.

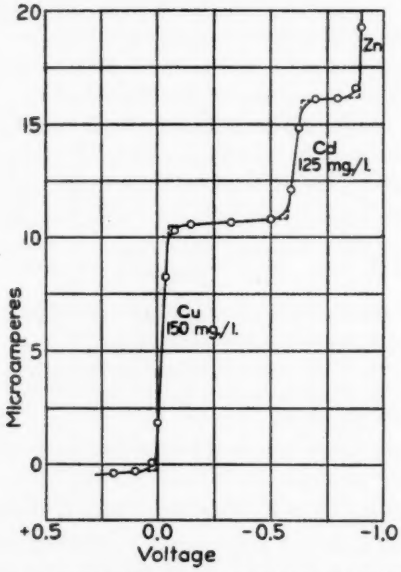

FIG. 1. *Current-voltage curve for copper and cadmium.*

Two methods were used for estimating the wave height and thus for determining the concentration of the electro-reducible substance in solution. One is illustrated in Fig. 1, namely, drawing the best straight line through each "plateau" and then measuring the differences in height. The other is the method of Müller and Petras (4), which reduces the necessary measurements of the current to that obtained for two fixed voltages. A linear calibration curve is obtained by plotting the differences between these two values for solutions of various known concentrations against the concentration. Using the 9 and 150 ohm shunts the concentrations of copper corresponding to 1 mm. of wave height were found to be 1.83 and 0.156 mg. of copper per litre, respectively. The corresponding values for cadmium were 3.30 and 0.250 mg. per litre, respectively.

Experimental Results

Effect of Amount of Zinc Dust Added to the N.T.O. and of Time of Agitation on the Removal of Copper and Cadmium and on the Final pH of the Solution

Fig. 2 shows the effect of agitation time on the deposition of copper from the N.T.O. solution for runs with zinc dust additions varying from 0.125 to 0.500 gm. per litre. It is evident that addition of 0.125 gm. of zinc dust per litre is insufficient to remove more than about half of the copper from solution; the addition of 0.250 gm. of zinc dust per litre reduces the copper to about 5 mg. per litre, while additions of 0.375 gm. per litre and 0.500 gm. per litre reduce the copper content to less than 1 mg. per litre in 50 and 35 min., respectively.

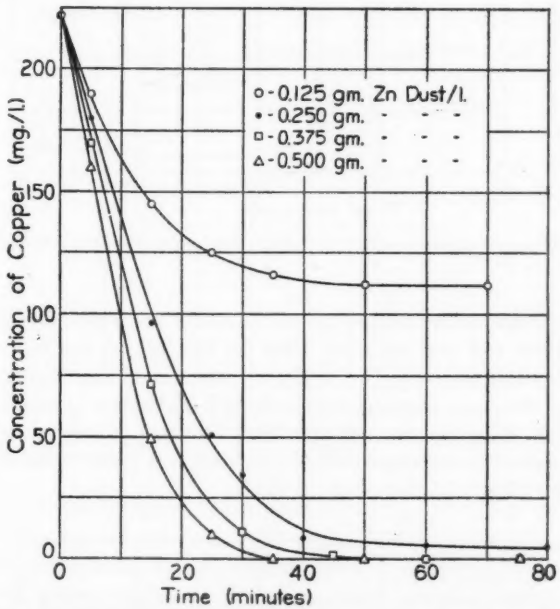

FIG. 2. *Effect of amount of zinc dust added and agitation time on the precipitation of copper.*

The corresponding graphs (Fig. 3) showing the effect of time of agitation and the amount of zinc dust added on the deposition of cadmium indicate that with the 0.125 and 0.250 gm. additions of zinc per litre of solution there is only a slight temporary deposition of cadmium and that redissolving of this soon takes place. With the 0.375 gm. per litre addition the precipitation of cadmium is somewhat greater, but partial redissolving occurs rapidly, this effect continuing more slowly after about 40 min. The 0.500 gm. per litre addition of zinc dust reduces the cadmium concentration to a minimum of 7 mg. of cadmium per litre in 45 min. and, after this, redissolving of cadmium

occurs at a very slow rate. In a later series of experiments it was found that addition of 0.65 gm. of zinc dust reduced the cadmium to 2 mg. per litre.

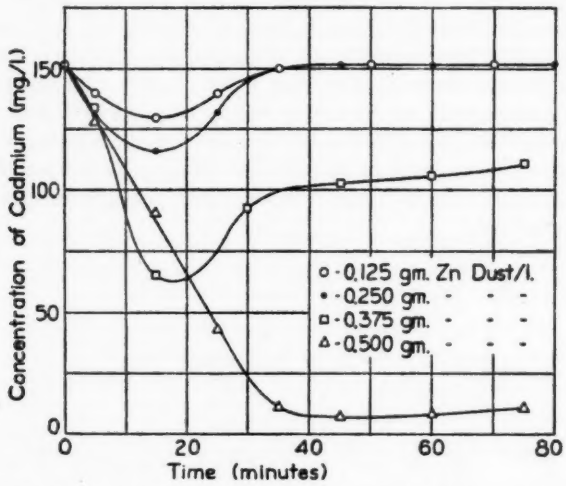

FIG. 3. *Effect of amount of zinc dust added and agitation time on the precipitation of cadmium.*

Fig. 4 gives the corresponding curves showing the effect of the amount of zinc dust added and the agitation time on the pH of the N.T.O. solution. Starting with a solution of pH = 5.27, the addition of zinc dust raises the pH progressively, the value in each case reaching a maximum in about 40 minutes. The maximum value for the addition of 0.500 gm. of zinc dust per litre is pH = 5.60, which is the same within experimental error as the value for the addition of 0.375 gm. of zinc dust per litre.

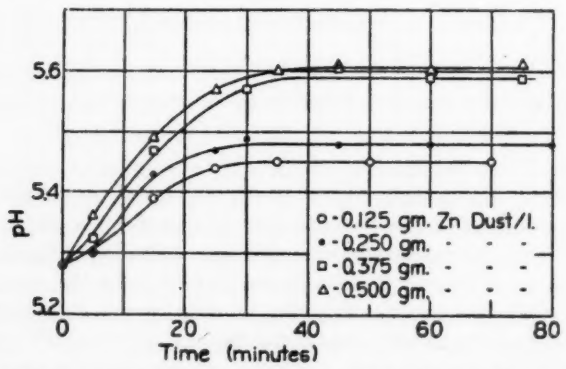

FIG. 4. *Effect of amount of zinc dust added and agitation time on the pH of the N.T.O. solution.*

Considering the above results, it was decided to fix the time of agitation of the N.T.O. solution with zinc dust at 45 min. in all further experiments.

Replicate determinations of the above-mentioned curves agreed very well as to the horizontal portions and as well as could be expected along the vertical portions where time is an important factor.

Fig. 5 shows the effect of the amount of zinc dust added on the precipitation of the cadmium from the N.T.O. solution. The time of agitation in all cases was 45 min. It is apparent that there is no permanent precipitation of cadmium if less than 0.250 gm. of zinc dust per litre is added and that an addition of 0.500 gm. per litre is necessary to reduce the cadmium content to 7 mg. per litre.

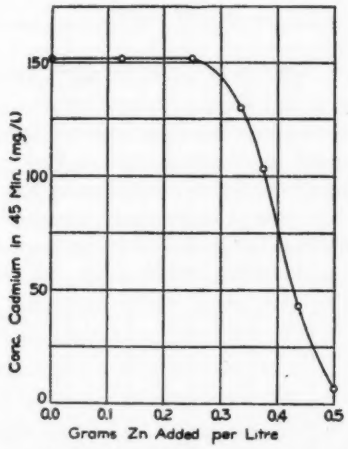

FIG. 5. *Effect of amount of zinc dust added on final concentration of cadmium.*

The Effect of the Initial pH of the N.T.O. Solution

Fig. 6 gives the effect of the initial pH of the N.T.O. solution on the precipitation of cadmium at 40° C. on addition of 0.5 gm. of zinc dust per litre and an agitation time of 45 min. It shows that, provided the initial pH of the solution is between the limits 5.1 and 3.6, there was no noticeable effect on the final concentration of cadmium. Below pH of 3.5 there is a rapid increase in the cadmium remaining in the solution at the end of 45 min., and at a pH of 2 the final concentration of cadmium reaches 96 mg. per litre (initial, 152 mg. per litre). When the initial pH was below 3.0, bubbles of hydrogen came off at such a rate as to make the solution appear opalescent*. Initial pH values down to 2 did not affect the precipitation of copper materially.

* *In a private communication Mr. S. P. Lowe, Superintendent of Research, Hudson Bay Mining and Smelting Company, states that hydrogen is evolved from the solution during the treatment with zinc dust providing the pH is below 6. The noticeable evolution of hydrogen gas at the higher pH values under plant conditions is probably due to the fact that the proportion of zinc dust used in plant practice is several times the largest amount used in our experiments. The large excess is considered necessary in order to remove arsenic, antimony, and cobalt, the presence of which lowers the current efficiency during the deposition of the zinc.*

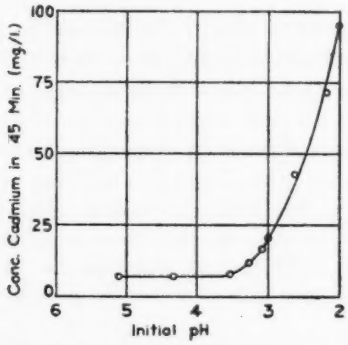

FIG. 6. *Effect of the initial pH of the N.T.O. solution on the precipitation of cadmium.*

The Effect of Air on the Removal of Cadmium and Copper

It is well known in practice that during the later stages of the agitation of the N.T.O. solution with zinc dust, cadmium tends to redissolve in the liquid. (This effect is illustrated in all the curves of Fig. 3.) The authors are not aware that any explanation of this phenomenon has been proposed. As the effect of aeration on the rate of underwater corrosion of base metals, such as iron, in the neutral and acid zone is well known, an experiment was made to determine the effect of bubbling air through the N.T.O. solution after the

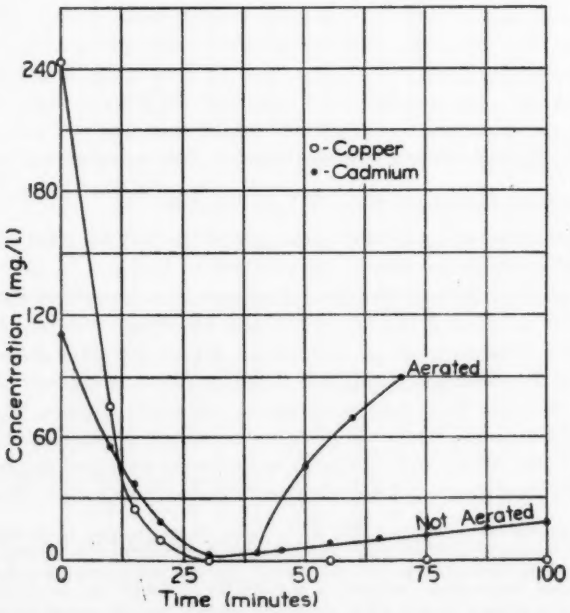

FIG. 7. *Effect of aeration of the N.T.O. solution on the redissolving of cadmium.*

minimum cadmium content of the solution had been reached. The solution was treated with 0.65 gm. of zinc dust per litre at 40° C. in the usual way. The copper content was reduced to zero and the cadmium content to a minimum of 2 mg. per litre. In a second run a rapid current of air was passed through the solution after the initial 40 min. and the determination of copper and cadmium continued at intervals. Fig. 7 shows the curve obtained for the copper and cadmium content of the solution compared with the normal curve obtained without aeration. This shows very rapid redissolving of cadmium in the aerated liquid, the concentration reaching 90 mg. per litre after aeration for 30 min. (initial, 110 mg. of cadmium per litre). No redissolving of copper was observed.

Discussion

Assuming that we are dealing with the direct displacement of copper and cadmium in solution by zinc, the addition of 125 mg. of zinc dust (100% pure) per litre should precipitate 55% of the copper present, as against 50% actually precipitated, an efficiency of 90% of the theoretical at the end of 50 min. agitation. The 250 mg. addition of zinc dust represents about 10% in excess of the requirements for precipitating all the copper, and as at the end of 60 min. 98% of the copper and none of the cadmium remains precipitated, the efficiency is about 89% of the theoretical. For the addition of 375 mg. of zinc dust the precipitation in 60 min. represents 100% of the copper and 30% of the cadmium present which is only 68% of the theoretical, although if one considers the points of maximum precipitation of copper (100%) and cadmium (57%) separately the efficiency is 74% of the theoretical. Similarly, for 500 mg. addition of zinc dust the precipitation in 45 min. represents 100% of the copper and 95.4% of the cadmium, giving an efficiency of 62.5%.

The behaviour of the cadmium is in agreement with what would be expected on the basis of the electrochemical theory of corrosion (5, pp. 21–41; 6). The single electrode potentials involved are: copper = +0.34; H = ±0.00; cadmium = −0.40; and zinc = −0.76 volts. Considering the three metals, we have the possibility of three electrical couples, Cu–Zn (1.1 volts), Cd–Zn (0.36 volts) and Cu–Cd (0.74 volts). The initial effect of adding zinc dust to a solution containing copper and cadmium is to deposit both the metals on the zinc dust, the deposition of copper predominating. Soon, however, the copper–cadmium couple operates, with the result that the latter dissolves and no further effective precipitation of cadmium occurs. If there is insufficient zinc dust to precipitate all the copper, the cadmium already precipitated will redissolve during the later stages of the precipitation of copper. This is illustrated by the two smallest additions of zinc dust (Figs. 2 and 3). With the two larger proportions of zinc dust, the copper is completely precipitated, and the slow redissolving of cadmium cannot be due to the replacement of copper in the solution by cadmium. Under the conditions of the writers' experiments, hydrogen gas is not evolved in any considerable quantities during the precipitation of cadmium unless the pH is quite low (below about 3 to 3.5),

i.e., unless the hydrogen ion concentration is high. A factor preventing the evolution of hydrogen during the precipitation of cadmium is the high overvoltage of hydrogen on copper (which on polished copper varies from 0.5 to 1.2+ volts), while the overvoltage for the deposition of metal on metal is small. Thus hydrogen behaves as if it were more anodic than cadmium, and the latter may be almost completely replaced by zinc on the acid side of the neutral point. The effect of the hydrogen ion concentration on the removal of cadmium is illustrated in Fig. 6.

The slow redissolving of cadmium shown in the 0.375, 0.500, and 0.65 gm. additions of zinc (see Figs. 3 and 7) is apparently due to depolarization by oxygen. The film of hydrogen, which plates out on the precipitated copper in contact with precipitated cadmium through the displacement of hydrogen ions by cadmium, prevents further action. This film, which may be atomic and is at any rate quite reactive, is removed by the oxygen in solution, and the rate of redissolving of cadmium is therefore determined by the rate at which oxygen is supplied; hence the rapid increase in the redissolving of cadmium during aeration (Fig. 7). When the hydrogen ion concentration is high enough, molecular hydrogen is evolved and the process continues spontaneously in the absence of oxygen.

Acknowledgments

The authors are indebted to Mr. S. P. Lowe, Superintendent of Research of the Hudson Bay Mining and Smelting Company, for suggesting this problem, for supplying the N.T.O. solution and the zinc dust, as well as for constructive criticism of the preliminary manuscript. They also wish to thank Dr. J. W. T. Spinks and Mr. M. R. Foran for helpful suggestions in connection with the experimental work.

References

1. CARR, J. D. and REIKIE, M. K. T. Trans. Can. Inst. Mining Met. 38 : 287-310. 1935.
2. HEYROVSKY, J. Phil. Mag. (Ser. 6) 45 : 303-315. 1923.
3. KOLTHOFF, I. M. and LINGANE, J. J. Chem. Revs. 24(1) : 1-94. 1939.
4. MÜLLER, R. H. and PETRAS, J. F. J. Am. Chem. Soc. 60(12) : 2990-2993. 1938.
5. SPELLER, F. N. Corrosion. McGraw-Hill Book Company, Inc., New York and London. 1926.
6. WHITNEY, W. R. J. Am. Chem. Soc. 25(4) : 394-406. 1903.

THE DECOMPOSITION OF BENZOYL PEROXIDE IN BENZENE[1]

By J. H. McClure[2], R. E. Robertson[3], and A. C. Cuthbertson[4]

Abstract

A kinetic study has been made of the decomposition of benzoyl peroxide in benzene. Kinetic data for this study have been obtained from three separate sets of measurements. Rate measurements from evolved carbon dioxide and direct iodometric measurements of peroxide are in good agreement. Alkalimetric determinations of the product, benzoic acid, have also been made during the course of the reaction.

Gravimetric determinations show that the total evolved carbon dioxide from the reaction is a function of the temperature, and indicate that the mechanism involves two parallel fast reactions, one of which evolves one mole of carbon dioxide per mole of peroxide and the other two moles of carbon dioxide per mole of peroxide. The latter reaction predominates at higher temperatures.

A kinetic analysis is included and provides for a slow reaction involving the rupture of the peroxide bond, followed by free radical reactions.

$$C_6H_5COOOCOC_6H_5 \xrightarrow{\text{Slow}} 2C_6H_5COO \begin{cases} \xrightarrow{\text{Fast}} CO_2 \\ \xrightarrow{\text{Fast}} 2CO_2 \end{cases}$$

The secondary free radical reactions would probably form hydrogen radicals, but there is evidence to support the view that these hydrogen radicals are not eliminated by mutual termination.

The reaction is first order and the energy of activation was found to be 31,000 cal. per mole.

Introduction

In this investigation, which deals with the decomposition of benzoyl peroxide in benzene, an attempt will be made to formulate a kinetic mechanism by which the reaction takes place. The obvious complexity of the reaction has made it advisable to obtain measurements not only for the rate of disappearance of the peroxide, but also for the rate of formation of the products, notably carbon dioxide and benzoic acid. Other investigators (1–3, 6, 8–13, 27), with two exceptions (4, 18), have studied the decomposition of benzoyl peroxide not from the standpoint of rate but by analysis of the end-products obtained after refluxing the peroxide in various solvents for protracted periods of time, or by heating the solid peroxide with sand as a diluent.

As early as 1864, Brodie (2, 3) found that benzoyl peroxide mixed with sand decomposed to yield one mole of carbon dioxide per mole of peroxide. Orndorff and White (21) noted the decomposition of benzoyl peroxide in boiling benzene with the liberation of carbon dioxide, while Lippmann (19) found that no reaction took place until the solution was heated in a closed tube to a temperature somewhat over 100° C. The latter obtained one mole of carbon

[1] *Manuscript received in original form March 2, 1942, and as revised, April 27, 1942. Contribution from the Department of Chemistry, Mount Allison University, Sackville, N.B.*

[2] *Instructor, 1940–1941.*

[3] *Instructor, 1941–1942.*

[4] *Professor of Chemistry.*

dioxide per mole of peroxide, benzoic acid, benzoic anhydride, and diphenyl. Diphenyl was produced when the compound was heated with sand, and he concluded that the benzene was an inert medium.

In the years following 1924, Gelissen and Hermans (8–13) and later Böeseken (1) carried out many investigations on the decomposition of diacyl peroxides in ordinary solvents. In the case of benzoyl peroxide their earlier investigations led them to assume that benzene or other solvents reacted with the benzoyl peroxide according to the following scheme, which involved a main and side reaction.

$$\text{I}\quad C_6H_5COOOCOC_6H_5 + C_6H_6 \longrightarrow C_6H_5COOH + C_6H_5C_6H_5 + CO_2 \qquad \text{Main}$$

$$\text{II}\quad C_6H_5COOOCOC_6H_5 + C_6H_6 \longrightarrow C_6H_5COOC_6H_5 + C_6H_6 + CO_2 \qquad \text{Side}$$

It is to be noted that according to this mechanism one mole of carbon dioxide is evolved per mole of benzoyl peroxide. The analysis of the end-products of the reaction showed the following substances present:— benzoic acid (partly in the form of an ester), 37.6%; diphenyl, 16.7%; phenyl-benzoate, 1.67%; quaterphenyl, 2.2%; a residue amounting to 29.2% (having a composition: C, 80%; H, 6%; O, 14%); and a small quantity of terphenyl. In addition 20.8% of carbon dioxide was evolved. It will be seen later that the assumption that this percentage corresponds to one mole of carbon dioxide per mole of peroxide is probably in error. Experiments carried out by us show that had the reaction been run to completion rather than for seven hours, the percentage of carbon dioxide would have varied even more strikingly from their theoretical value of 18.2%. In another communication (15) the above authors found that when benzoyl peroxide was heated above its melting point either with or without a solvent the decomposition proceeded according to the following scheme:

$$C_6H_5COOOCOC_6H_5 \longrightarrow C_6H_5C_6H_5 + 2CO_2$$

The same authors, as well as others (26), proved that benzene participated in the reaction because di-*p*-chlorobenzoyl peroxide, on decomposition in benzene yielded *p*-chlorobiphenyl rather than *p,p*-dichlorobiphenyl. Similarly *m,m*-dinitrobenzoyl peroxide gave 3-nitrodiphenyl rather than 3,3-dinitrodiphenyl. Hey (16) gives further proof of the reaction of the peroxide with the solvent.

Some years later Böeseken and Hermans (1) summarized the possible reactions as follows:

$$\text{I}\quad C_6H_5COO\,.\,OCOC_6H_5 \longrightarrow C_6H_5C_6H_5 + 2CO_2$$

$$\text{II}\quad C_6H_5COO\,.\,OCOC_6H_5 \longrightarrow C_6H_5COOC_6H_5 + CO_2$$

$$\text{III}\quad C_6H_5COO\,.\,OCOC_6H_5 \longrightarrow C_6H_5C_6H_4COOH + CO_2$$

$$\text{IV}\quad C_6H_5COO\,.\,OCOC_6H_5 + C_6H_6 \longrightarrow C_6H_5COO\,.\,OCOH + C_6H_5C_6H_5$$

$$\downarrow$$

$$C_6H_5COOH + CO_2$$

According to this scheme, the main path of the decomposition proceeds by Reactions I and II. Proof of the presence of phenylbenzoic acid has been established by Wieland (27).

The question whether a free radical mechanism is involved has been discussed by Wieland and co-workers (27) and by Hey and Waters (17) and others (24). The first have maintained that the presence of free radicals was both unlikely and unnecessary to explain the decomposition of peroxides. The same opinion was also held by Reynhart (22) and implied by Böeseken and Hermans (1). Hey and Waters (17) do not consider the evidence against the presence of free radicals conclusive, and propose that the initial stage of decomposition is the formation of free radicals as set forth below:

$$C_6H_5COOOCOC_6H_5 \longrightarrow C_6H_5^{\cdot} + C_6H_5COO^{\cdot} + CO_2,$$

followed by such reactions as:

$$C_6H_5COO^{\cdot} + C_6H_6 \longrightarrow C_6H_5COOH + C_6H_5^{\cdot}$$
$$C_6H_5^{\cdot} + C_6H_6 \longrightarrow C_6H_5C_6H_5 + H^{\cdot}$$
$$C_6H_5^{\cdot} + C_6H_5C_6H_5 \longrightarrow C_6H_5C_6H_4C_6H_5 + H^{\cdot}$$
$$C_6H_5COO^{\cdot} + H^{\cdot} \longrightarrow C_6H_5COOH$$
etc.

The reactivity of the phenyl radical is well known, and it is expected that if it were produced a reaction with solvent molecules would occur. Certainly the formation of ter- and quater-phenyl could easily be explained on the basis of the production of free phenyl radicals.

Although this reaction is obviously complicated an attempt will be made in what follows to make a kinetic analysis, bearing in mind certain facts which a preliminary study indicated were fundamental. So far as the measurement of the rate of the reaction is concerned, this may be accomplished either by titration of liberated iodine with thiosulphate according to the method of Gelissen and Hermans (14); or the evolution of carbon dioxide will provide a continuous method if a simple stoichiometric relation can be found between the concentration of benzoyl peroxide and evolved carbon dioxide at any time. From the mechanisms suggested one is led to believe that one mole of carbon dioxide is evolved for every mole of benzoyl peroxide decomposed. Careful measurements indicate, however, that the number of moles of carbon dioxide evolved is a function of the temperature; that is to say, at a temperature in the vicinity of 65° C., one mole of carbon dioxide is produced per mole of peroxide while at the temperature of boiling benzene, about one and one-half moles of carbon dioxide are evolved. These facts need to be incorporated into any kinetic mechanism. It is essential to express the same mechanism in terms of more than one set of measurements, i.e., in terms of evolved carbon dioxide, thiosulphate titres of the peroxide and perhaps alkali titres of the benzoic acid. If all these data can be satisfactorily correlated, it can confidently be felt that it approximates the truth.

A difficulty will be experienced in the study of this reaction unless the reactants are of a high degree of purity. This difficulty is substantiated by some

of the earlier investigators (8). Brown (4) finds a short induction period for this reaction. We found none in experiments where carefully purified materials were used, though our mechanism does not exclude the possibility of one. The fact that the rate is, to a good approximation, first order indicates that if an induction period is present it is very short and relatively unimportant.

Kinetic Analysis

The increase per mole in the evolution of carbon dioxide with rising temperature is explained by assuming that there is a slow initial decomposition of the benzoyl peroxide molecule into two benzoyl radicals (17; 25, p. 776), followed by two fast parallel reactions yielding one and two moles of carbon dioxide respectively.

$$(1)\ C_6H_5COOOCOC_6H_5 \xrightarrow[k_1]{\text{Slow}} 2C_6H_5COO \begin{cases} \xrightarrow{k_2} CO_2 \text{ products} & \text{Path 1} \\ \xrightarrow{k_3} 2CO_2 \text{ products} & \text{Path 2} \end{cases}$$

The initial decomposition may be followed by such fast free radical reactions as:

$$(2)\ C_6H_5COO^{\cdot} + C_6H_5COO^{\cdot} \longrightarrow C_6H_5COOC_6H_5 + CO_2 \qquad \text{Path 1}$$

$$(3)\ 2C_6H_5COO^{\cdot} + C_6H_6 \longrightarrow C_6H_5COOH + C_6H_5C_6H_5 + CO_2$$

$$C_6H_5COO \,.\, OCOC_6H_5 \longrightarrow 2C_6H_5COO^{\cdot} \longrightarrow 2CO_2 + 2C_6H_5^{\cdot} \quad \text{Path 2 (i)}$$

$$C_6H_5^{\cdot} + C_6H_6 \longrightarrow C_6H_5C_6H_5 + H^{\cdot} \quad \text{(ii) Collision with solvent} \quad (a)$$

$$^{*}C_6H_5^{\cdot} + C_6H_6 \longrightarrow C_6H_6 + C_6H_5^{\cdot} \quad \text{(ii) Collision with solvent} \quad (b)$$

$$C_6H_5^{\cdot} + C_6H_5C_6H_5 \longrightarrow C_6H_5C_6H_4C_6H_5 + H^{\cdot} \quad \text{(iii)}$$

Free Radical Termination Reactions

$$H^{\cdot} + C_6H_5^{\cdot} \longrightarrow C_6H_6 \qquad \text{(iv) } (a)$$

$$H^{\cdot} + H^{\cdot} \longrightarrow H_2 \qquad \text{(iv) } (b)$$

$$C_6H_5^{\cdot} + C_6H_5^{\cdot} \longrightarrow C_6H_5C_6H_5 \qquad \text{(iv) } (c)$$

If M is the concentration of peroxide at any time t, the rate may be expressed:

$$\frac{-dM}{dt} = k_1 M.$$

If x be the fraction of a mole of peroxide changing by Path 2, then

$$\frac{x}{1-x} = \frac{k_3}{k_2},$$

and C_t, the total number of moles of carbon dioxide evolved at any time t, will be:

$$= (1 + x)\ (A + M),$$

where A is the initial peroxide concentration. Substituting for x

$$C_t = \frac{(2k_3 + k_2)}{(k_3 + k_2)}(A - M) = y\frac{(2 + K)}{(1 + K)},$$

* *Transfer reaction.*

where $K = \frac{k_2}{k_3}$ and y is the amount of peroxide decomposed at time t. Hence the total evolved carbon dioxide is expressed by

$$C_\infty = \frac{2 + K}{1 + K} \cdot A.$$

This permits the evaluation of K and hence y at any time t. Our original kinetic equation in terms of evolved carbon dioxide now becomes

$$\frac{dy}{dt} = k_1 (A - y).$$

The iodometric titration of the peroxide at any time t will yield directly the value of M. Thus we have available two separate methods for determining the value of k_1. The results so obtained at three temperatures are given in Table IV. The rate of production of benzoic acid may be controlled by k_1; hence values of k_1 calculated from alkalimetric determinations of the acid are included.

Experimental

Materials

Benzene: Analar benzene from B.D.H. was kept over metallic sodium and redistilled before use.

Benzoyl peroxide: This product was obtained from B.D.H. and contained 25% of water. It was dissolved in chloroform and twice precipitated by pouring into twice the volume of methyl alcohol according to the method suggested by Gattermann (7, p. 126).

Acetone: In iodometric determinations of the peroxide it is necessary to use pure acetone (5, 14) since the commercial product will frequently free iodine from potassium iodide. The titration medium should be as low in water content as the experimental conditions will permit, otherwise low titration values will be obtained.

Apparatus

Reactions were carried out in an all-glass apparatus. In the volume measurements of carbon dioxide care was exercised in the design of the apparatus so that the volume above the liquid phase was small. The carbon dioxide evolved was collected over mercury in a gas burette so constructed that small volumes measured during the initial stages of the reaction were read with an accuracy comparable to that obtained with larger volumes in the later stages. For the titration experiments a 250 ml. distilling flask with a sealed-on condenser (30 cm. long) was used. Samples were removed through a capillary tube immersed in the solution. Gravimetric determinations were carried out by attaching to the upper end of the condenser a trap immersed in a freezing mixture, followed by a standard carbon dioxide absorption train.

Procedure

In experiments involving the evolution of carbon dioxide a measured quantity of benzene was placed in the apparatus and allowed to stand for 15 min. to ensure that it had reached the correct temperature. The glass

mercury seal was then raised and a small quantity of benzoyl peroxide quickly added. Following the replacement of the mercury seal, a three-way stop-cock attached between the reflux condenser and the measuring tube was allowed to remain open to the air for five minutes in order to permit any trapped air to reach the correct temperature and pressure. In titration determinations, samples were cooled to 25° C. before the 5 ml. samples were pipetted out. Owing to the insolubility of benzoic and phenylbenzoic acid, care was needed to obtain the true end-point, in alkalimetric titrations. Actual tests with phenyl benzoate showed that under the conditions of titration, no appreciable hydrolysis took place.

Data

In Table I are shown typical yields of carbon dioxide per mole of benzoyl peroxide as obtained from measurements of evolved gas.

TABLE I

YIELDS OF CARBON DIOXIDE

Run No.	Temp., °C.	Conc., moles per litre		
		Benzoyl peroxide	CO_2	C_∞/A
13	66	0.0684	0.0732	1.07
14	66	0.112	0.121	1.08
15	66	0.168	0.181	1.07
8	72.5	0.069	0.087	1.25
18	72.5	0.139	0.174	1.25
7	72.5	0.208	0.260	1.25
9	78	0.0690	0.0999	1.45
11	78	0.110	0.167	1.51
12	78	0.166	0.247	1.49

Evidence set forth in Table II shows that the reaction is first order by comparing the times to half-value for varying concentrations of peroxide in benzene at three temperatures.

Some typical kinetic data regarding carbon dioxide evolution, thiosulphate titres, and alkali titres, at three temperatures, and calculated values of k_1 are detailed in Table III. A summary of the above values and ratios of $\frac{k_2}{k_3}$ is set forth in Table IV.

The corresponding yields of carbon dioxide obtained gravimetrically per mole of benzoyl peroxide are given in Table V.

Discussion

The suggestion that benzoyl peroxide decomposes so as to produce free radicals is not new. Arguments both in favour and against this proposal have been cited in the introduction. As Walker and Wild point out (24)

TABLE II

A COMPARISON OF TIMES TO HALF-VALUE

Run	Conc. peroxide, moles/litre	Time to half-value, hr.	
		Calc.	Obs.
Temp., 66° C.			
15	0.168	21.2	20.2
13	0.0684	25.7	27.0
14	0.112	27.4	23.0
Temp., 72.5° C.			
7	0.208	11.2	11.0
8	0.0695	9.6	9.1
18	0.139	10.1	9.8
Temp., 78° C.			
9	0.0690	5.05	4.9
11	0.110	4.9	4.7
12	0.165	5.3	4.3

TABLE III

TYPICAL KINETIC DATA FROM THREE DIFFERENT SETS OF MEASUREMENTS

Run	14		31		32	
Initial conc., moles/litre	0.112		0.140		0.140	
Time, hr.	Vol. CO_2, ml., S.T.P.	$k_1 \times 10^2$, $hr.^{-1}$	Titre with 0.101 *N* $Na_2S_2O_3$	$k_1 \times 10^2$, $hr.^{-1}$	Titre with 0.367 *N* $Ba(OH)_2$	$k_1 \times 10^2$, $hr.^{-1}$
Temp., 66° C.						
0	0.0	–	14.30	–	0.0	–
4	7.5	2.46	12.90	2.6	0.90	2.9
7	12.8	2.48	12.05	2.5	1.60	3.40
13	22.2	2.50	10.20	2.6	2.45	3.5
23	37.0	2.71	7.80	2.6	3.90	2.90
28	44.0	2.84	7.05	2.5	4.5	3.0
46.5	62.9	3.3	4.80	2.4	5.9	2.8
∞	80	–	–	–	8.0	–
Temp., 78° C.						
Run	11		29		24	
Initial conc., moles/litre	0.1104		0.140		0.140	
0	0	–	14.30	–	0	–
2	27.0	13.8	11.20	12.5	1.50	10.8
5	56.7	14.1	7.30	13.4	2.90	10.1
7	71.5	14.5	5.45	13.8	3.80	10.8
9	82.0	14.5	–	–	4.5	10.3
12	93.5	13.5	2.6	14.2	5.4	10.3
∞	112	–	–	–	7.30	–

TABLE IV

FIRST ORDER CONSTANTS AND RATIOS OF k_2/k_3 AT THREE TEMPERATURES

Run	k_1, hr.$^{-1}$	$\frac{k_2}{k_3}$
Temp., 66° C.		
13	2.70×10^{-2}	13.2
*14	2.53×10^{-2}	12.2
15	3.13×10^{-2}	11.8
Av. CO_2	2.78×10^{-2}	Av. 12.4
†31 Iodometric	2.45×10^{-2}	
‡32 Alkalimetric	2.76×10^{-2}	
Temp., 72.5° C.		
8	7.20×10^{-2}	2.94
18	6.87×10^{-2}	2.95
7	6.17×10^{-2}	3.08
Av. CO_2	6.74×10^{-2}	Av. 2.99
†Iodometric	5.09×10^{-2}	
‡Alkalimetric	4.97×10^{-2}	
Temp., 78° C.		
9	1.37×10^{-1}	1.23
11	1.41×10^{-1}	0.95
12	1.30×10^{-1}	1.06
Av. CO_2	1.36×10^{-1}	Av. 1.08
†Iodometric	1.35×10^{-1}	
‡Alkalimetric	1.05×10^{-1}	

* *This value is an average k_1, from a larger set of data than presented in Table III.*

† *These values were obtained by titrating iodine freed by potassium iodide from 5 ml. samples of benzoyl-peroxide–benzene solution. There is good reason to believe the value of 5.09×10^{-2} at 72.5° is somewhat low.*

‡ *These values were obtained by titration of the products benzoic and phenyl benzoic acid with barium hydroxide.*

TABLE V

GRAVIMETRIC DETERMINATIONS OF CARBON DIOXIDE

Run	Temp., °C.	Conc. peroxide, gm.	CO_2, gm.	C_∞/A expressed, moles
27	78	1.7857	0.4784	1.47
19	72.5	0.800	0.1773	1.25
31	66	3.5853	0.6980	1.07

the RH scheme suggested by Gelissen and Hermans (8–13) and in modified form by Böeseken and Hermans (1) summarizes in convenient form and comprehensive manner the different kinds of end-products of the thermal decomposition without suggesting the real mechanism through which such products are produced.

On the other hand, the free radical mechanism proposed by Hey and Waters (17) will be in agreement with our experimental data if provision be made for the variation of total evolved carbon dioxide per mole of benzoyl peroxide with temperature. In order to reconcile the characteristics of free radical reactions with the relative slowness of the above decomposition (half-life = 10 hr. at 72.5° C.) it is necessary to postulate a mechanism having two steps.

The first step in the decomposition is concerned with the slow production of free benzoyl radicals. Since the subsequent free radical reactions are very rapid, the rate actually measured (25, p. 776) will be that rate at which the peroxide bond is broken, and, as Rice (23) points out, the minimum value for the activation energy may correspond to the energy required for the rupture of the peroxide bond. Acetyl peroxide has the same kind of a peroxide bond. It is significant therefore that Walker and Wild (24) found the activation energy for the unimolecular decomposition of acetyl peroxide in toluene at 80° C. to be 31,000 cal. per mole, compared with 31,000 cal. per mole found by us from values of k_1 obtained from average carbon dioxide data, Table IV. The energy of activation for benzoyl peroxide in benzene calculated from the data of Kamenskaja and Medwedew (18) at 75° and 85° was found to be 30,000 cal. This may indicate that the rate of bond rupture is nearly independent of the nature of the "R" groups associated with the peroxide linkage.

Since the total moles of carbon dioxide evolved per mole of benzoyl peroxide is a function of the temperature (Fig. 1), there must be two types of secondary reactions. The first, predominating at lower temperatures, yields one mole of carbon dioxide per mole of peroxide, together with benzoic, phenylbenzoic acids and various aryl esters. The second, amounting to 50% of the total at 78° C., yields two moles of carbon dioxide per mole of peroxide together with phenyl radicals which in turn react with solvent and other molecules. The presence of such reactive particles will most easily explain the formation of polyphenyls and higher molecular weight esters found by Gelissen and Hermans.

According to our results data from the evolution of carbon dioxide and alkalimetric titration indicate that at 66° C. Equations (2) and (3), Path 1, are in a ratio of roughly 3 to 1. As the temperature rises, there must be an increasing tendency for the relatively unstable benzoyl radicals to decompose further to yield carbon dioxide and a highly reactive phenyl radical. The extent of this tendency is expressed by the variation of $\frac{C_\infty}{A}$ with temperature.

Both the mechanism suggested by Hey and Waters (17) and that presented lead to the production of free hydrogen radicals. Proof that there is no

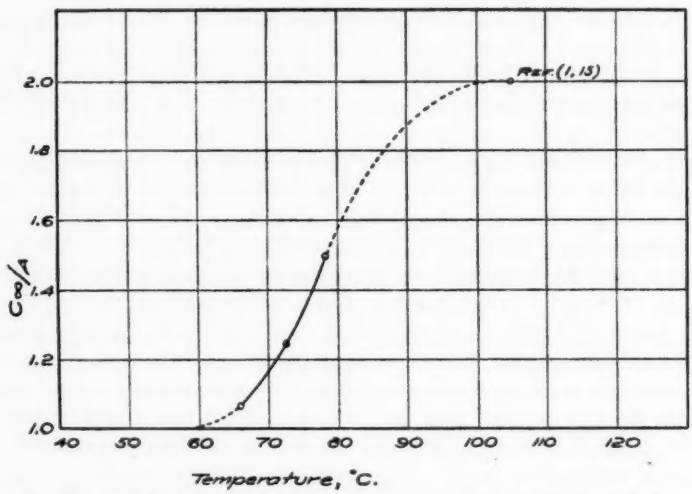

FIG. 1. *Relation between C_∞/A and temperature. Dotted portions of the line are assumed.*

appreciable union of these to form molecular hydrogen as suggested in Equation (iv, *b*) was obtained by the gravimetric determination of evolved carbon dioxide. The values of C_∞/A calculated from these determinations are given in Table V and are in substantial agreement with those obtained from volume measurements (Table I). Were hydrogen produced, the gravimetric values would certainly be lower. Elsewhere (26) it has been shown that phenyl radicals do not combine in solution to give diphenyl. On the basis of this evidence, Reactions (iv *b*, *c*) must occur only rarely if at all. It seems highly probable therefore, that a reaction between the aforesaid radicals (iv*a*) must take place with particular ease. The presence of comparatively large amounts of residue containing oxygen may be explained if it is assumed that the phenyl radicals react with the ester and acid radicals.

References

1. BÖESEKEN, J. and HERMANS, P. H. Ann. 519 : 133-139. 1935.
2. BRODIE, B. C. Ann. 129 : 282-286. 1864.
3. BRODIE, B. C. Ann. Suppl. 3 : 200-226. 1864–1865.
4. BROWN, D. J. J. Am. Chem. Soc. 62(10) : 2657-2659. 1940.
5. CONANT, J. B. and KIRNER, W. R. J. Am. Chem. Soc. 46(1) : 232-252. 1924.
6. FICHTER, F. and FRITSCH, A. Helv. Chim. Acta, 6 : 329-336. 1923.
7. GATTERMANN, L. Laboratory methods of organic chemistry. Revised by H. Wieland. The Macmillan Company, New York and London. 1932.
8. GELISSEN, H. and HERMANS, P. H. Ber. 58 : 285-294. 1925.
9. GELISSEN, H. and HERMANS, P. H. Ber. 58 : 476-479. 1925.
10. GELISSEN, H. and HERMANS, P. H. Ber. 58 : 479-481. 1925.
11. GELISSEN, H. and HERMANS, P. H. Ber. 58 : 764-765. 1925.
12. GELISSEN, H. and HERMANS, P. H. Ber. 58 : 765-770. 1925.
13. GELISSEN, H. and HERMANS, P. H. Ber. 58 : 770-772. 1925.

14. GELISSEN, H. and HERMANS, P. H. Ber. 59 : 63-68. 1926.
15. GELISSEN, H. and HERMANS, P. H. Ber. 59 : 662-666. 1926.
16. HEY, D. H. J. Chem. Soc. 1934 : 1966-1969. 1934.
17. HEY, D. H. and WATERS, W. A. Chem. Revs. 21(1) : 169-208. 1937.
18. KAMENSKAJA, S. and MEDWEDEW, S. Acta Physicochim. U.R.S.S. 13 : 565-586. 1940.
19. LIPPMANN, E. See Reference (8).
20. MOELWYN-HUGHES, E. A. Kinetics of reactions in solution. The Clarendon Press, Oxford. 1933.
21. ORNDORFF, W. R. and WHITE, J. Am. Chem. J. 15(5) : 347-356. 1893.
22. REYNHART, A. F. A. Rec. trav. chim. 46 : 68-71. 1927.
23. RICE, F. O. and RICE, K. The aliphatic free radicals. Johns Hopkins Press, Baltimore. 1935.
24. WALKER, O. J. and WILD, G. L. E. J. Chem. Soc. 1937 : 1132-1136. 1937.
25. WATERS, W. A. Trans. Faraday Soc. 37 : 770-781. 1941.
26. WIELAND, H., POPPER, E., and SEEFRIED, H. Ber. 55 : 1816-1834. 1922.
27. WIELAND, H., SCHAPIRO, S., and METZGER, H. Ann. 513 : 93-106. 1934.

THE SAP OF THE BIRCH TREE, *BETULA PAPYRIFERA* MARSH.

I. THE AMYLASE SYSTEM[1]

BY E. BOIS[2] AND W. O. CHUBB[3]

Abstract

The amylase system of birch sap consists of a cellobiogenic amylase and most probably a glucogenic amylase. The optimum conditions of pH and temperature are pH 5.5 at 4° C. to 6.3 at 60° C. The maximum production of cellobiose occurred at a temperature of 50° C. at the optimum pH for this temperature. The optimum conditions for the production of glucose were pH 5.5 and a temperature of 50° C.

It is felt that these new facts throw some additional light on the constitution of starch, and that possibly birch sap might serve as a source of cellobiose, which has heretofore only been prepared commercially by hydrolysis of cellulose acetate.

Introduction

In 1833 Payen isolated a concentrate of barley diastase and recognized it as belonging to a new class of substances now called enzymes. Since then a large number of papers have been published concerning this and other amylases.* However, very few dealt with the possibility of the production, by amylases, of sugars other than maltose, the presence or kinetics of the amylases chiefly being investigated. Among the few are notably those by Bailey (2), Bois and Chubb (3), Bois and Nadeau (4), Brown and Millar (7)†, Falk and McGuire (9), Gottschalk (11), Gray (12), Ling (8, 16, 17)‡, Pringsheim and Leibowitz (21), Sjöberg (22), Tallarico (25), Vinson (26), Wrede (20, p. 257; 28), Wülfert (29).

It was decided to investigate the sap of a tree, since, on the assumption that conditions would parallel those in the sugar maple sap, it was likely to be a ready aqueous solution of any amylases present (5). The white birch was chosen because its sap runs very plentifully in the spring.

Experimental

In preliminary tests, mixtures were made up of 1% soluble starch solution and fresh birch sap in the presence of toluene. The mixtures were buffered at various pH values, allowed to react at different temperatures, and the speed of hydrolysis of the starch was followed by means of the iodine–starch coloration. It was found that the variations in the rate of hydrolysis of the

[1] *Manuscript received March 2, 1942.*

Contribution from the Biochemistry Laboratory, Faculty of Science, Laval University, Quebec, Que.

[2] *Professor of Biochemistry.*

[3] *Holder of a Bursary under the National Research Council of Canada, 1937-38; Quebec Provincial Bureau of Scientific Research, 1938-39, 1939-40, first half of 1940-41. At present, Chemist, St. Lawrence Sea Products Company, Quebec, Que.*

* *See Walton (27) for a comprehensive bibliography up to 1925.*

† *See also Walton (27), Abstract No. 288.*

‡ *See Walton (27), Abstracts Nos. 307, 312, 314.*

starch, caused by varying the pH and temperature of the samples, were reproducible. Mixtures in which a boiled sap was used exhibited no hydrolysis at the end of two weeks, nor did mixtures containing sap that had been heated to 80° C. for 15 min.

It was concluded therefore that the sap contains an amylase system which is completely inactivated on being heated to 80° C. for 15 min.

Products of the Hydrolysis of Starch by Birch Sap

It was found that two reducing sugars in the sap reacted with the phenylhydrazine reagent to give glucosazone and cellobiosazone. The osazones were identified by means of their melting points and mixed melting points (using osazones prepared directly from the pure sugars). With a set of standard thermometers, the melting points obtained by means of the capillary tube method were 201° C. for the glucosazone and 194° to 197° C. for the cellobiosazone. The reducing sugar that gave glucosazone did not react with Seliwanoff's reagent and was therefore not fructose or invert sugar (ketose), nor did it react in the cold with the phenylhydrazine reagent (mannose). It was therefore concluded that it is glucose.

The absence of sucrose was verified by means of a test with invertase.

To ascertain what sugars were produced in the hydrolysis of starch by the sap *in vitro* a mixture was made of dialysed sap and starch solution and phosphate buffer solution to buffer the whole at a pH of about 6.0. (Toluene was added to this, as to all subsequent digestion mixtures, as preservative.) The crystal forms of the osazones obtained from the sugars produced were the same as those from the sugars in the sap.

Properties of the Birch Sap Amylolytic System

The amylolytic activity of the sap was estimated at different temperatures and pH values by determining the amount of total reducing sugars (calculated as dextrose) produced in 24 and 48 hr.

The digestion samples were at first made up of a mixture of 4 parts sap, 4 parts 1% soluble starch solution, 1 part phosphate buffer solution and, of course, an excess of toluene; later the proportions were changed to 5 : 5 : 1. Blanks in which water replaced the starch solution were run with each determination and, at first, second blanks containing water instead of sap were also used but they were found to be unnecessary. For any one series of determinations, at different pH values and temperatures, homogeneous portions of sap and starch solution were used throughout.

The amounts of reducing sugars were determined in a 5 ml. sample using the Luff-Schoorl method (6, p. 830; 18) and, as noted above, calculated as milligrams dextrose increase.

The pH values of the samples were in all cases measured (using a glass electrode) after, and in some before, the digestion period.

It must be noted in this connection that some trouble was encountered in the buffering of the digestion mixtures. During the 48 hr. reaction period

the pH was found to vary considerably, in some cases as much as 0.3 pH units. It was ascertained that these variations were partly due to the soft glass of the containers, and it is probable that some part was due to the loss of free carbon dioxide (which was contained in the sap). But other, unknown, factors also probably contribute to the variation.

The temperatures were constant to about $\pm$ 0.25° C. except the temperature of 23° (that of the room) which varied not more than about 2°.

In this manner the amylolytic activity of the sap was estimated at pH values of 4.8, 5.5, 6.1, and 7.3 at temperatures of 6°, 23°, 50°, and 60° C.

The results of these determinations (expressed as increase in reducing sugars as a function of the pH at each temperature) gave curves of the same form (see Fig. 1). It can be seen from these curves that the optimum pH, at all temperatures, was about 5.5. And, at this pH, the optimum temperature was about 50° C. Also, as would be expected, at the extremes of pH the activity was greatly diminished at the higher temperatures. At a pH of 7.3 and at 50° C. the sap was inactivated in less than 24 hr.

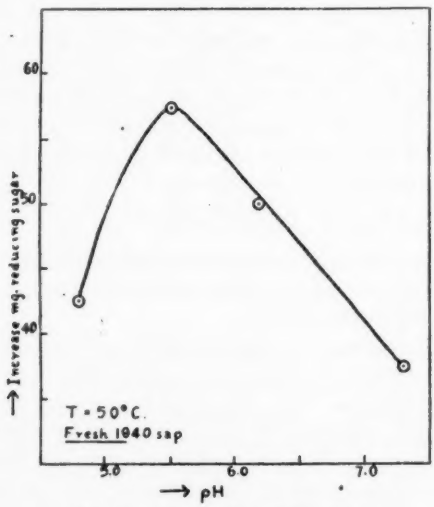

FIG. 1. *Amylolytic activity of sap.*

For a more complete investigation of the amylase system in the sap, it was necessary to estimate the production of glucose and cellobiose separately. Since both are reducing sugars it would be necessary to separate them, eliminate one or hydrolyse the cellobiose. An attempt at hydrolysis was first made but it was found that the necessary conditions would cause at least a partial hydrolysis of the dextrins formed during the starch degradation. After 17 hr. at 70° C., using the acid mixture standard for the cold inversion

of sucrose (1, p. 473, sec. XXXXIV, par. 23 (*c*)), cellobiose was only approximately 50% hydrolysed.

As it was reported by Skraup and König (23, 24) that cellobiose is not fermented by brewer's yeast, it was decided to try a method based on the elimination of the glucose in the mixture of sugars by alcoholic fermentation, leaving cellobiose as a residue that could be determined in the usual manner. A method that was satisfactory for the writers' purposes was worked out.

It consisted in pasteurization of the sample, after adjustment of the pH, addition of Fleischman's yeast, allowing to stand overnight at 37° C., addition of defecant (alumina cream), making to volume, filtering, and determining the cellobiose in an aliquot of the filtrate.

Using this method it was found that the rate of production of cellobiose, during the hydrolysis of starch in contact with the sap for 48 hr., varied with the pH and temperature of the mixture. This indicated the presence of a cellobiogenic amylase.

The rates of production of glucose and cellobiose by hydrolysis of starch by the sap were determined at various temperatures and pH values (reaction time, 48 hr.). Two series of determinations were made, one using a sap from the 1939 run, one year old, and the other using a fresh sap from the 1940 run.

In general form the activity curves were similar, as were also the optimum pH values and temperatures (see Figs. 2 and 3). For the production of glucose the optimum pH was 5.5 and, at this pH, a temperature of 50° C. For the production of cellobiose the optimum pH varied from 5.5 at 4° and 23° to 6.3 at 60° C. The variation between 23° and 37° C. was the greatest, being from 5.5 to 6.0. The greatest production of cellobiose occurred at 50° C., as in the case of glucose.

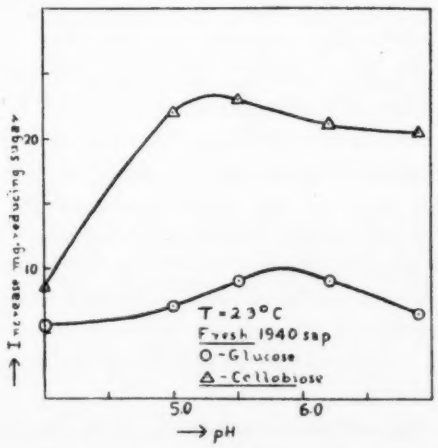

FIG. 2. *Production of sugars at 23°C.*

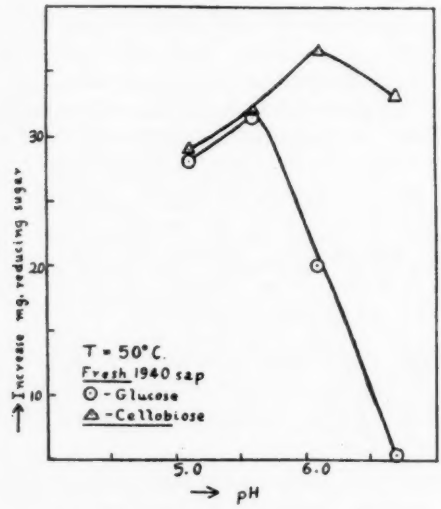

FIG. 3. *Production of sugars at 50° C.*

If the temperature-activity curves, at constant pH, are plotted (using the above data) it can be seen that the rates of production of both sugars fall off sharply once the optimum temperature, at each pH, has been passed. The curves show that at the higher pH values the cellobiogenic amylase is more resistant to inactivation by heat than the glucogenic amylase. At a pH of 6.8 the activity of the glucogenic amylase decreases at temperatures higher than 37° C. But at lower pH values, for example at 5.1, the activity of the cellobiogenic amylase decreases, after the optimum temperature for this pH has been reached, much faster than that of the glucogenic amylase.

The activities of the sap at pH 6.0 and 37° C. were determined from day to day during the entire 1940 run. There were no significant variations.

Oligosaccharases

It was thought possible that the glucose produced during the hydrolysis of starch, in contact with the sap, might have been due to an enzymatic hydrolysis of some of the cellobiose; therefore, tests were carried out to show the presence or absence of cellobiase. Fresh saps of the 1939 and 1940 runs were used. The test was carried out by supplying a substrate of cellobiose to the sap and determining the reducing power of the mixture before and after 48 hr. at 37° C. There was no increase in reducing power; consequently, cellobiase was absent.

Similar tests, using sucrose as substrate, were carried out, and these demonstrated the absence of invertase in the same saps.

Discussion

It has been shown above that the sap contains only two reducing sugars, glucose and cellobiose, and also that these are the sugars produced by the degradation of starch by the sap *in vitro*. It was concluded therefore that there is in the sap at least a cellobiogenic amylase.

But it might be expected that the glucose would be produced from the cellobiose, or perhaps from some other oligosaccharide, by enzymatic hydrolysis. It has been shown that the sap contains no cellobiase, so the glucose is not produced from the cellobiose. And since it has also been shown that there is no invertase in the sap, the glucose could not be produced from sucrose. The only other non-reducing disaccharides known that yield glucose only on hydrolysis are trehalose and isotrehalose. These sugars have, to date, been found in fungi only, where they are widely distributed. At the time it was not possible to investigate the possibility of the production of glucose from starch by means of a phosphorylase (see Hanes (13, 14)). Such an investigation is projected in this laboratory for the near future. In the meanwhile it is tentatively concluded that the glucose may be produced directly from starch by a glucogenic amylase.

One of the most widely accepted theories of the constitution of starch today envisages the molecule as made up of a large number of glucopyranose units joined into chains by maltose or α-linkages exclusively, these chains being joined together by some side linkages probably due to residual valencies. Haworth (15), who subscribes to this theory, bases his belief on (*a*) the fact that common diastases give only maltose and glucose by the hydrolysis of starch, and also on (*b*) the results of some acetolyzing experiments on a methylated starch. In the same way he claims to have proved that cellulose is made up of cellobiose units or alternating α- and β-linkages between the glucopyranose foundation units. Thus, maltose and cellobiose are regarded as the characteristic products of hydrolysis of starch and cellulose respectively.

Freudenberg (10) holds similar but slightly modified views. He considers the starch molecule as made up almost wholly of maltose units with only one other type of bond to every 20 or 25 maltose units. However, he is of the opinion that the maltose units are connected not in straight chains but in branched chains or branched rings. He advances as proof the results of some methylation experiments.

Myrbäck (19) favours the maltose linkage theory but emphasizes that any theory of the constitution of starch must account not only for its chemical behaviour but also, and in a satisfactory manner, for the action of the starch hydrolyzing enzymes.

It has been shown by the authors that cellobiose is produced by starch hydrolysis, and it has been shown by Bois and Nadeau (4) that both this sugar and sucrose are so produced. The claim is advanced therefore that any theory of the constitution of starch must not only account for the production of cellobiose, which differs from maltose only by the type of linkage between

the two glucopyranose units, but also for the production of sucrose, which differs fundamentally from maltose in structure, containing a fructo-furanose ring connected to a glucopyranose ring.

Moreover Freudenberg's modification cannot account for the production of these sugars, since a maximum of one in twenty, or 5% only, of sugars other than maltose can, according to his theory, be produced. And the authors have shown, as have Bois and Nadeau (5), that much greater yields of cellobiose and sucrose can be produced. For example, a yield of cellobiose, at 50° C. and a pH of 6.1, was obtained which was equivalent to a starch hydrolysis of about 33.3%. Bois and Nadeau obtained a yield of cellobiose, at 50° C. and a pH of 6.6, equivalent to a 45.4% hydrolysis, and a yield of sucrose, at 8° C. and a pH of 6.6, equivalent to a 40% hydrolysis.

It is submitted by the authors that these facts should be explained by a true theory of the constitution of starch.

References

1. Association of Official Agricultural Chemists. Official and tentative methods of analysis. 4th ed. A.O.A.C., Washington, D.C. 1935.
2. Bailey, E. M. J. Am. Chem. Soc. 34 (12) : 1706-1730. 1912.
3. Bois, E. and Chubb, W. O. Can. Chem. Process Ind. 22 : 322. 1938.
4. Bois, E. and Nadeau, A. Can. J. Research, B, 16 (4) : 114-120. 1938.
5. Bois, E. and Nadeau, A. Can. J. Research, B, 16 (4) : 121-133. 1938.
6. Brown, C. A. and Zerban, F. W. Sugar analysis. New York. 1941.
7. Brown, H. T. and Millar, J. H. J. Chem. Soc. 75 : 315-337. 1899.
8. Davis, B. F. and Ling, A. R. J. Chem. Soc. 85 : 16-29. 1904.
9. Falk, K. G. and McGuire, G. J. Gen. Physiol. 3 (5) : 595-609. 1921.
10. Freudenberg, K. Ann. Rev. Biochem. 8 : 81-107. 1939.
11. Gottschalk, A. Z. physiol. Chem. 152 : 132-135. 1926.
12. Gray, P. H. H. Can. J. Research, C, 17 (5) : 154-169. 1939.
13. Hanes, C. S. Proc. Roy. Soc. (London) B, 128 : 421-450. 1940.
14. Hanes, C. S. Proc. Roy. Soc. (London) B, 129 : 174-208. 1940.
15. Haworth, W. N. Chemistry & Industry, 58 (41) : 917-925. 1939.
16. Ling, A. R. J. Inst. Brewing, 9 : 446-461. 1903.
17. Ling, A. R. and Davis, B. F. J. Inst. Brewing, 8 : 475-495; discussion, 495-500. 1902.
18. Luff, G. and Schoorl, N. Rept. Proc. Ninth Session, Intern. Commission for Uniform Methods of Sugar Analysis. 1936.
19. Myrbäck, K. Ann. Rev. Biochem. 8 : 59-80. 1939.
20. Pringsheim, H. Chemistry of the saccharides. McGraw-Hill Book Company, Inc., New York and London. 1932.
21. Pringsheim, H. and Leibowitz, J. Ber. 58 : 1262-1265. 1925.
22. Sjöberg, K. Z. physiol. Chem. 162 : 223-237. 1927.
23. Skraup, Z. H. and König, J. Ber. 34 : 1115-1118. 1901.
24. Skraup, Z. H. and König, J. Monatsh. 22 : 1011-1036. 1901.
25. Tallarico, G. Arch. farmacol. sper. 7 : 27-48, 49-68. 1908.
26. Vinson, A. E. Botan. Gaz. 43 : 392-407. 1907.
27. Walton, R. P. A comprehensive survey of starch chemistry. Vol. 1. The Chemical Catalog, Inc., New York. 1928.
28. Wrede, H. Papier-Fabr. 27 (13) : 197-202. 1929.
29. Wülfert, K. Biochem. Z. 302 : 232-246. 1939.

CANADIAN JOURNAL OF RESEARCH

Notes on the Preparation of Copy

General:—Manuscripts should be typewritten, double spaced, and the *original* and *one copy* submitted. Style, arrangement, spelling, and abbreviations should conform to the usage of this Journal. Names of all simple compounds, rather than their formulae, should be used in the text. Greek letters or unusual signs should be written plainly or explained by marginal notes. Superscripts and subscripts must be legible and carefully placed. Manuscripts should be carefully checked before being submitted, to reduce the need for changes after the type has been set. All pages should be numbered.

Abstract:—An abstract of not more than about 200 words, indicating the scope of the work and the principal findings, is required.

Illustrations

(i) *Line Drawings:*—Drawings should be carefully made with India ink on white drawing paper, blue tracing linen, or co-ordinate paper ruled in *blue* only. Paper ruled in green, yellow, or red should not be used. The principal co-ordinate lines should be ruled in India ink and all lines should be of sufficient thickness to reproduce well. Lettering and numerals should be of such size that they will not be less than one millimetre in height when reproduced in a cut three inches wide. If means for neat lettering are not available, lettering should be indicated in pencil only. All experimental points should be carefully drawn with instruments. Illustrations need not be more than two or three times the size of the desired reproduction, but the ratio of height to width should conform with that of the type page. The *original drawings* and one set of small but clear *photographic copies* are to be submitted.

(ii) *Photographs:*—Prints should be made on glossy paper, with strong contrasts; they should be trimmed to remove all extraneous material so that essential features only are shown. Photographs should be submitted *in duplicate;* if they are to be reproduced in groups, one set should be so arranged and mounted on cardboard with rubber cement; the duplicate set should be unmounted.

(iii) *General:*—The author's name, title of paper, and figure number should be written on the back of each illustration. Captions should not be written on the illustrations, but typed on a separate page of the manuscript. All figures (including each figure of the plates) should be numbered consecutively from 1 up (arabic numerals). Reference to each figure should be made in the text.

Tables:—Titles should be given for all tables, which should be numbered in Roman numerals. Column heads should be brief and textual matter in tables confined to a minimum. Reference to each table should be made in the text.

References should be listed alphabetically by authors' names, numbered in that order, and placed at the end of the paper. The form of literature citation should be that used in this Journal and titles of papers should not be given. All citations should be checked with the original articles. Each citation should be referred to in the text by means of the key number.

The *Canadian Journal of Research* conforms in general with the practice outlined in the *Canadian Government Editorial Style Manual*, published by the Department of Public Printing and Stationery, Ottawa.